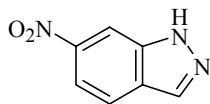


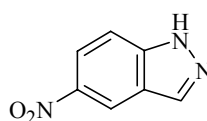
## PART B. ACCOMPLISHMENTS

### CHAPTER 4. CHEMISTRY

The results from earlier work established that the nucleophilic aromatic substitution reaction between 1-methyl-4-chloropyridinium iodide (**115**) and 7-nitroindazole (**68**) leads to product formation. However, the reaction conditions generated demethylation products, the yields were low and the regiochemistry could be assigned only tentatively. In this study, our first aim was to assign unambiguously the regiochemistry to the previously synthesized compound (**108** or **110**). The second part of the study involved the investigation of the mechanism of the nucleophilic aromatic substitution reaction of 7-NI (**86**) with **115** with one goal being the synthesis of both isomeric precursors to the “prodrugs” of 7-NI, **85** and **86**. We also explored the possibility of applying this chemistry as a general method to synthesize the “prodrugs” of 2 other structurally related and biologically relevant compounds, 6-nitroindazole [6-NI (**122**)] and 5-nitroindazole [5-NI (**123**)].



**122**



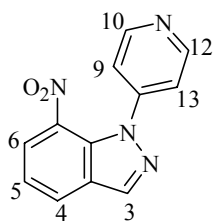
**123**

Finally a nucleophilic aromatic substitution reaction was carried out with indazole (**89**) to understand better the effect of the nitro group on the mechanism and the regiochemistry of the reaction. The results obtained from the indazole chemistry helped to provide unambiguous assignment of the regiochemistry to the previously reported 4-indazolyipyridine compound obtained via the 4-fluoropyridine chemistry described in Scheme 37.

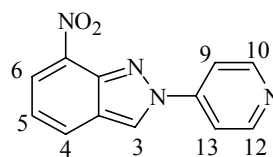
## 4.1. SYNTHESIS OF THE 7-NI “PRODRUGS”

### 4.1.1. CHARACTERIZATION OF THE PREVIOUSLY OBTAINED PRODUCT (108 or 110)

Assignment of the regiochemistry to the product of the reaction shown in Scheme 41 was not possible using standard  $^1\text{H}$  NMR techniques since the other isomer was not available for comparison at this point. The mass spectrum did not provide information leading to an unambiguous assignment either. Therefore we decided to attempt an NMR experiment utilizing the Nuclear Overhauser Effect (NOE). A new technique, DPFGE-NOE (**D**ouble **P**ulsed **F**ield **G**radient **S**pin **E**cho-**N**OE) was used. This new technique does not require the subtraction of the irradiated spectrum from the non-irradiated spectrum as in the case of a regular NOE experiment. Thus, the desired effects can be recorded without interference from other signals.<sup>168</sup> In this technique, pulse field gradients are introduced into the pulse sequence. The combining pairs of selective pulses with pulse field gradients are used as a method to offer high-quality selective excitation.<sup>169</sup>



**108**



**110**

First a standard  $^1\text{H}$  NMR spectrum was obtained in  $\text{DMSO-d}_6$  (Figure 4).

<sup>168</sup> Braun, S., Kalinowski, -O., Berger, S. (1998) *150 and more basic NMR experiments*, pp.460-463 Wiley, New York.

<sup>169</sup> Stott, K., Keeler, J., Van, Q.N., Shaka, A.J. (1997) One-dimensional NOE experiments using pulsed field gradients. *J. Magn. Reson.* **125**, 302-324.

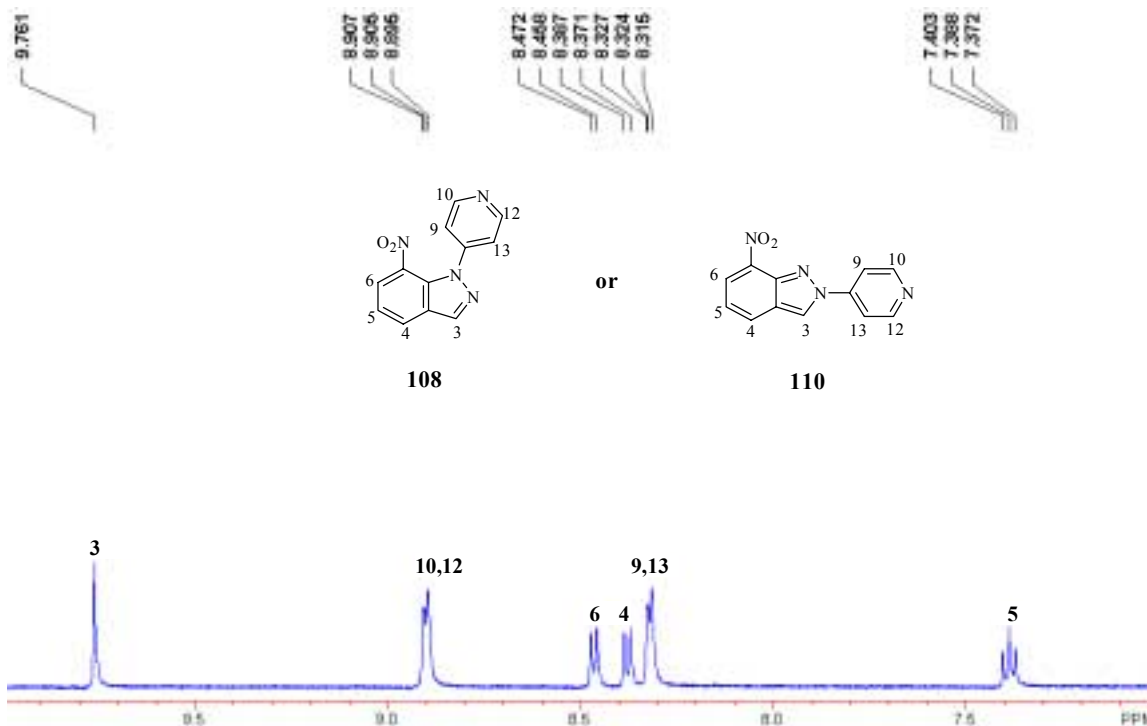


**Figure 4.**  $^1\text{H}$  NMR spectrum (instrument frequency = 400 MHz) of the product obtained from the reaction shown in Scheme 41.

We assigned the most downfield signal (9.8 ppm) to the proton at C3. Since C3 is doubly bonded to a nitrogen atom, it will be expected to be less shielded. Also, as required, this signal is a singlet. The next upfield signal at 8.9 ppm, the first of the two signals integrating for 2 protons, was assigned to the protons at C10 and C12 again because they are attached to a carbon doubly bonded to an electronegative nitrogen atom. The other signal at 8.3 ppm integrating to 2 protons was assigned to the protons at C9 and C13. The most upfield signal at 7.4 ppm was assigned to the proton at C5 which gives an overlapping doublet of doublets, merging to form a triplet, resulting from its *ortho* coupling to the protons at C4 and C6. The signals at 8.4 ppm and 8.5 ppm were assigned tentatively to the protons at C6 and C4.

Next, in an DPGSE-NOE experiment, the signal of the proton at C3 was irradiated. Due to their close proximity in space to the proton at C3, an enhancement for the signal of the protons as C9 and C13 was expected for the *2H* isomer. This enhancement was not expected for the *1H* isomer where the protons at C9 and C13 are

located far from the proton at C3. We obtained the following spectrum upon irradiation of the signal of the proton at C3 (Figure 5).

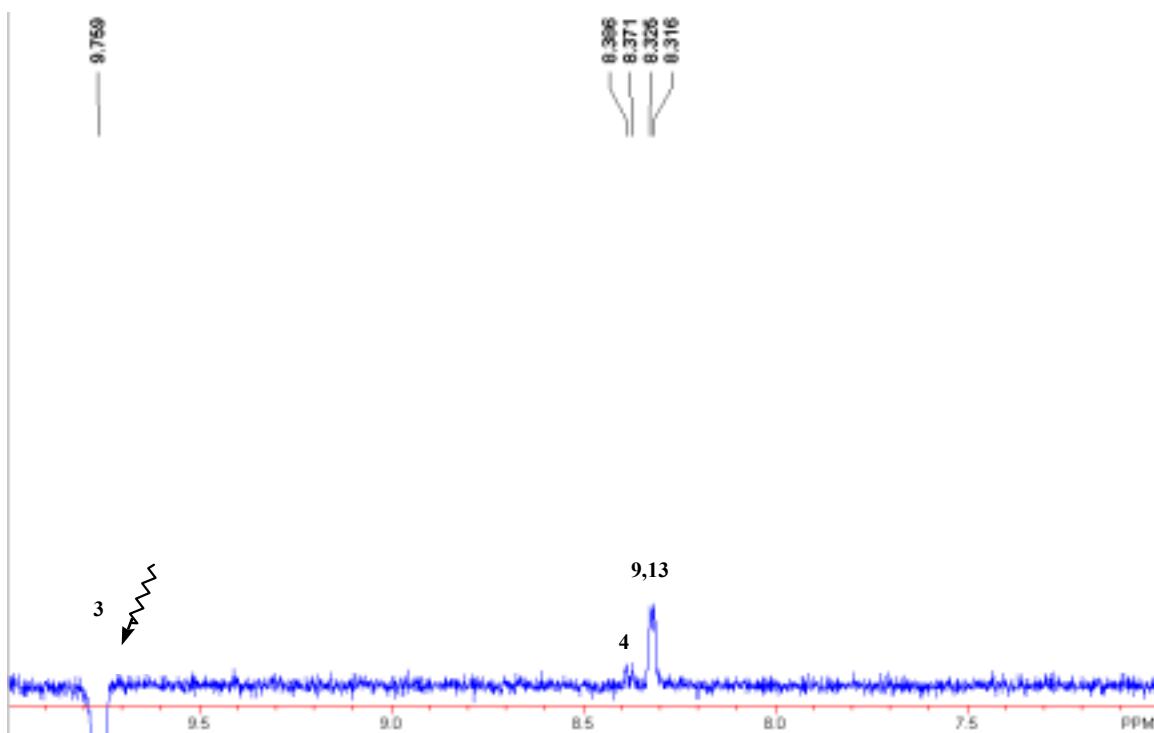
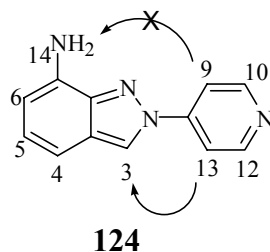


**Figure 5. Irradiated  $^1\text{H}$  spectrum for the product obtained from the reaction shown in Scheme 41.**

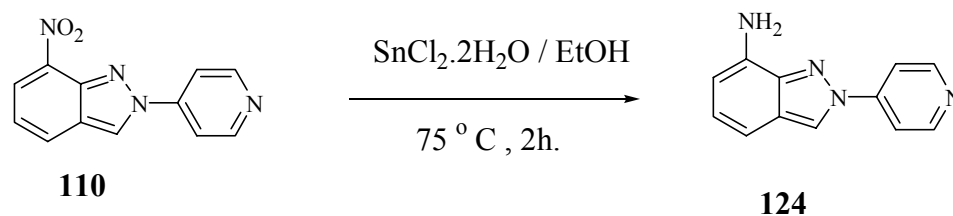
There was indeed an enhancement for the signal of the protons at C9 and C13, which enabled us to assign unambiguously the regiochemistry of the product as the *2H* isomer **110**. In addition to this enhancement, we also observed an enhancement for the signal we had tentatively assigned to the proton at C4. This enhancement confirmed the assignment since the proton at C6 is not close enough in space to the proton at C3 for an NOE effect but the proton at C4 is. These findings demonstrated that the previous tentative assignment was incorrect.

In order to confirm our results obtained from the DPGSE-NOE experiment, we first reduced the nitro group at C7 position to an amino group. In this case, irradiation of protons at C9 and C13 were expected to result in an enhancement for the proton at C3 but not the protons on the amino nitrogen N14.



The reduction of 4-(7-nitroindazol-2-yl)pyridine (**110**) was attempted using  $\text{SnCl}_2 \cdot 2\text{H}_2\text{O}$  which was reported to be a selective reducing agent for the nitro group.<sup>170</sup> The reaction was carried out in ethanol at 75 °C for 2 hours (Scheme 44).

**Scheme 44. Selective reduction of the nitro group.**



The reaction mixture was extracted with ethyl acetate and analyzed by GC-MS. The TIC tracing showed an  $\text{M}^+$  peak at  $m/z = 240$  corresponding to the starting material and a second minor peak at  $m/z = 210$  and another peak which we did not attempt to characterize. The 210 Da ion corresponds to the  $\text{M}^+$  of the desired amine **124**. The product was isolated in low yield using column chromatography. However, as we only needed enough material to perform the NOE experiment, optimization of the reaction conditions was not pursued. The full characterization of the compound was not possible due to the small amount of compound available. The  $^1\text{H}$  NMR spectrum of the compound was taken in  $\text{DMSO-d}_6$  and showed the presence of the amino protons as a singlet at 5.5 ppm (Figure 6).

<sup>170</sup> Bellamy, F.D., Ou, K. (1984) Selective reduction of aromatic nitro compounds with stannous chloride in non acidic and non aqueous medium. *Tet. Lett.* **25**, 839-842.

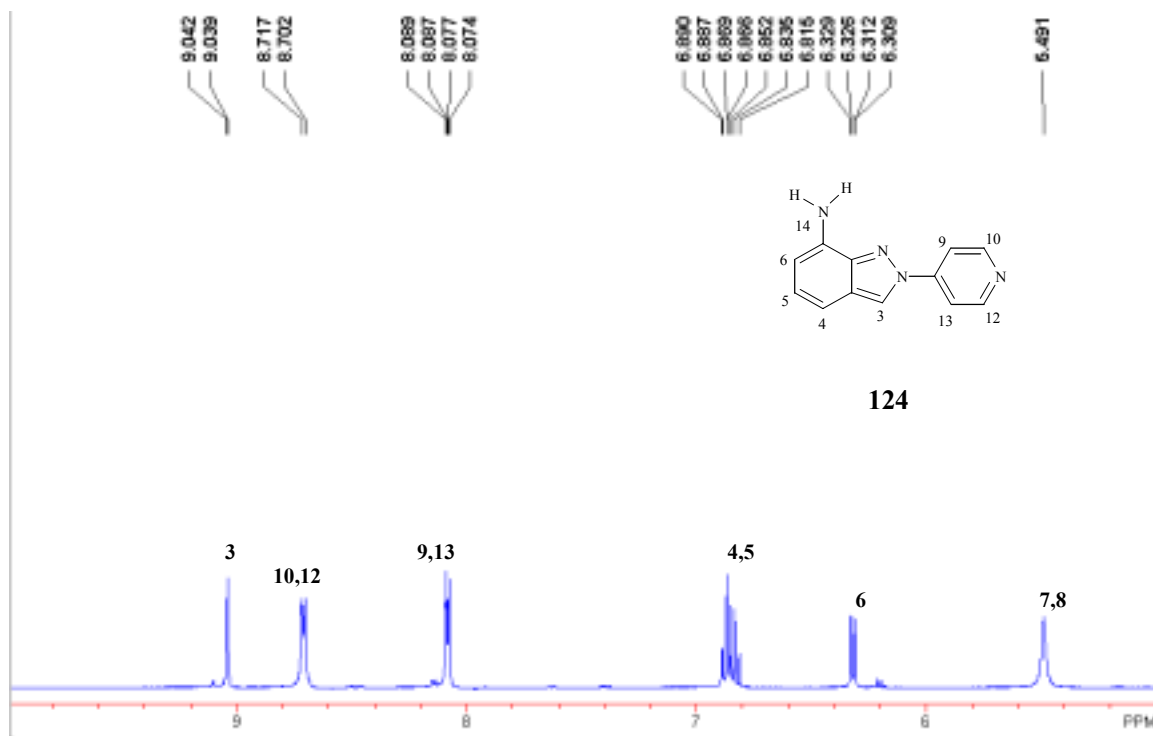
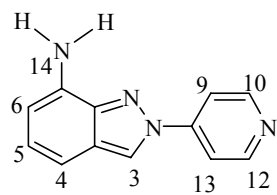


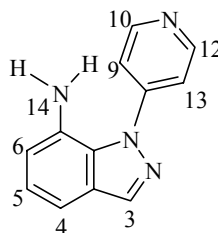
**Figure 6.** <sup>1</sup>H NMR spectrum (instrument frequency = 400 MHz) of the product obtained from reaction shown in Scheme 44.

The 3 most downfield signals were assigned as described for compound **110**. The signal at 6.3 ppm was assigned to the proton at C6 since it was shielded by the electron donating effect of the amino group via resonance. The overlapping signals integrating for 2 protons at 6.9 ppm were assigned to the protons at C4 and C5 which were expected to be shifted downfield compared to the signal of the proton at C6 since they are not affected as much by the electron donating effect of the amino group.

The NOE experiment was run in DMSO-d<sub>6</sub>. The signals for the protons assigned to C9 and C13 were irradiated. Consistent with the *2H* isomer **124**, an enhancement was observed of the signal for the proton attached to C3 but not the signal for the protons at the amino nitrogen N14 (Figure 7). Furthermore, irradiation of the signal for the proton at C3 resulted in an enhancement of the signals for the protons at C9, C13 and C10, C12 which is in agreement with the first observation. The enhancement of the signal at 6.8 ppm confirmed the assignment of this signal to be due to the proton at C4 (Figure 8).



124



125

Formation of the *2H* isomer exclusively was unexpected since molecular modeling calculations carried out using MacSpartan molecular modeling software at the semi-empirical level (PM3) showed the electron density on both nitrogens to be the same and the 1-substituted product to be slightly more stable than the 2-substituted product. Presumably the presence of the nitro group at the 7 position causes steric hindrance for the incoming group disfavoring the N1 substitution. This may explain the formation of the *2H* isomer exclusively.

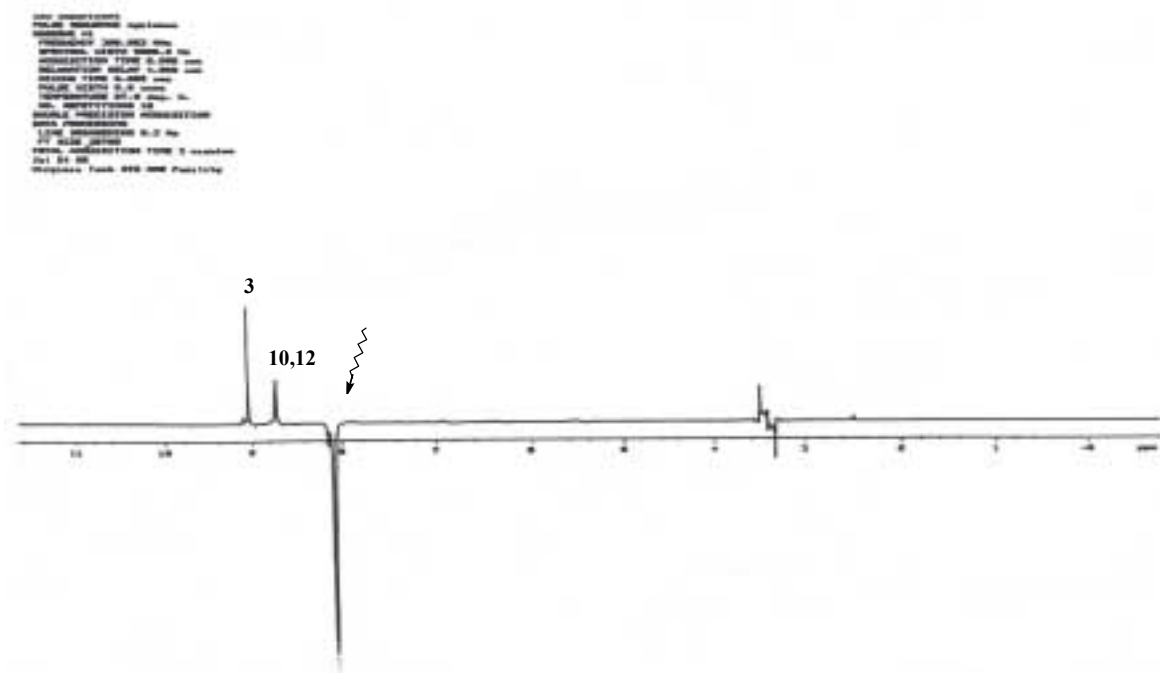


**Figure 7. Irradiation of the signal for the protons at C9 and C13 resulted in an enhancement for the signals of the protons at C3, C10 and C12.**

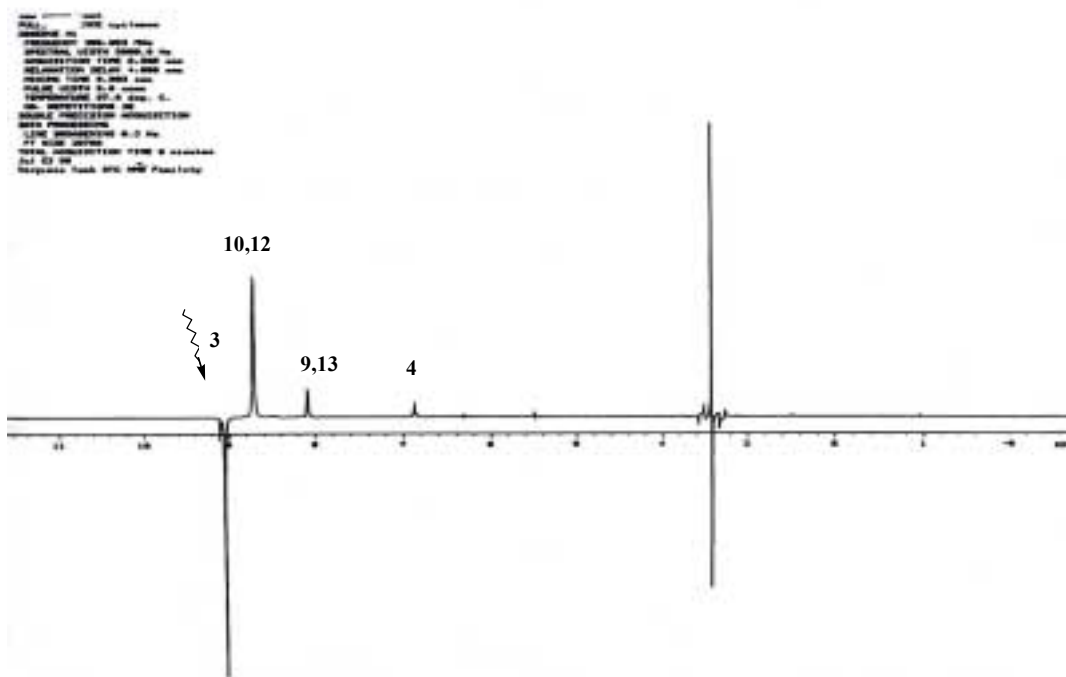


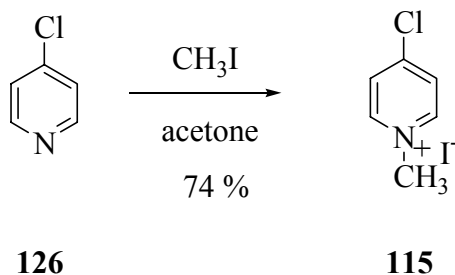
**Figure 8.** Irradiation of the signal for the proton at C3 resulted in an enhancement for the signals of the protons at C9, C10, C12, C13 and C4.

#### 4.1.2. REINVESTIGATION OF THE COUPLING REACTION OF 115 WITH 7-NI (68)

At this point we decided to reexamine the nucleophilic aromatic substitution reaction shown in Scheme 41 to confirm the previously reported results. The first step was the synthesis of the starting materials.

The synthesis of 4-chloro-1-methylpyridinium iodide (**115**) was achieved by treating free base **126** with  $\text{CH}_3\text{I}$  in acetone at room temperature (Scheme 45).

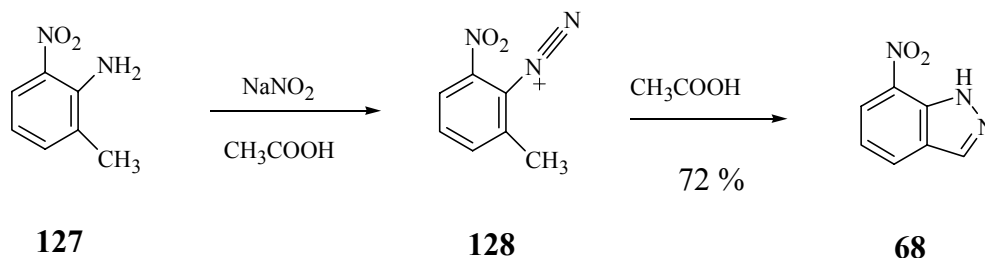
**Scheme 45. Methylation of 4-chloropyridine (126) by iodomethane gives the corresponding pyridinium salt 115.**



The product **115** had been reported as nearly white crystals.<sup>171</sup> However, in our hands, even after several crystallizations, green crystals were obtained. Therefore we reverted back to the original procedure<sup>169</sup> where **126** was allowed to react with neat  $\text{CH}_3\text{I}$  at 0 °C. This time, after crystallization from MeOH/ether, the crystals were nearly colorless.

The next step was the synthesis of the other starting material 7-NI (**68**). Although 7-NI was commercially available, it was expensive. Diazotization of 2-methyl-6-nitroaniline (**127**) followed by acid catalyzed cyclization was chosen as the pathway as reported in the literature (Scheme 46).<sup>172</sup> Compound **68** could be obtained in good yield.

**Scheme 46. Formation of 7-nitroindazole from 2-methyl-6-nitroaniline (127) via the diazotization reaction followed by acid catalyzed cyclization.**



<sup>171</sup> Sprague, R.H., Brooker, L.G.S. (1937) Studies in the cyanine dye series. IX. 4,4'-pyridocyanines and 4-pyrido-4'-cyanines *J. Am. Chem. Soc.* **59**, 2697-2699.

<sup>172</sup> Barbet, O., Minjat, M., Petavy, A., Paris, J. (1986) Phenyl urees derivees de l'indazole; recherche de l'activite anthelminthique, effet des substituants. *Eur. J. Med. Chem. -Chim. Ter.* **21**, 359-362.

After the synthesis of the starting materials we attempted the reaction illustrated in Scheme 41. GC-EIMS analysis of the ethyl acetate extract of the reaction mixture showed 3 principal peaks of interest (Figure 9). The first peak ( $M^+$  163 Da), corresponded to the starting material **68**. There were two additional peaks with  $M^+$  240 Da. The peak at 14.02 minutes was assigned to be the *2H* isomer **110** upon comparison with the synthetic standard. The other peak at 11.83 was tentatively assigned to be the other possible isomer **108**. The ratio of the two compounds was estimated as 1:5 from the GC-EIMS TIC tracing.

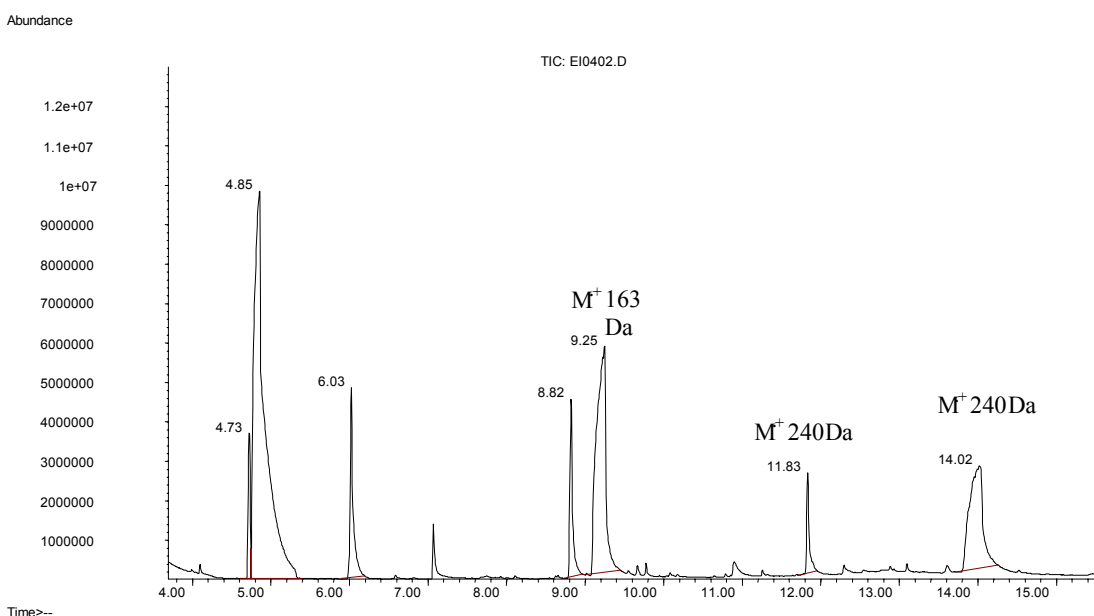


**Figure 9. GC-EIMS TIC tracings of the reaction shown in Scheme 51.**

The two products of interest were separated by column chromatography using silica gel as the stationary phase. Although both compounds appeared as single spots on TLC, the *1H* isomer (which had not been reported before) gave two peaks on the GC/MS TIC tracing. This compound was further purified by preparative TLC. The *1H* isomer was obtained in a very low yield which makes the synthetic utility of this reaction unfeasible for the synthesis of the *1H* isomer. Nevertheless, we could obtain a  $^1\text{H}$  NMR of the *1H* isomer. Together with the mass spectra this gave us the opportunity to compare the spectral features of the *1H* and the *2H* isomers **108** and **110**.

### 4.1.3. SPECTRAL FEATURES OF 4-(7-NITRO-INDAZOL-1-YL) AND 4-(7-NITRO-INDAZOL-2-YL)PYRIDINES

#### 4.1.3.1. COMPARISON OF THE $^1\text{H}$ NMR SPECTRA

Comparison of the  $^1\text{H}$  NMR spectra of the *1H* isomer **108** and the *2H* isomer **110** shows significant chemical shift differences for the protons attached to C3, C4, C9 and C13 (Figures 10 and 11).

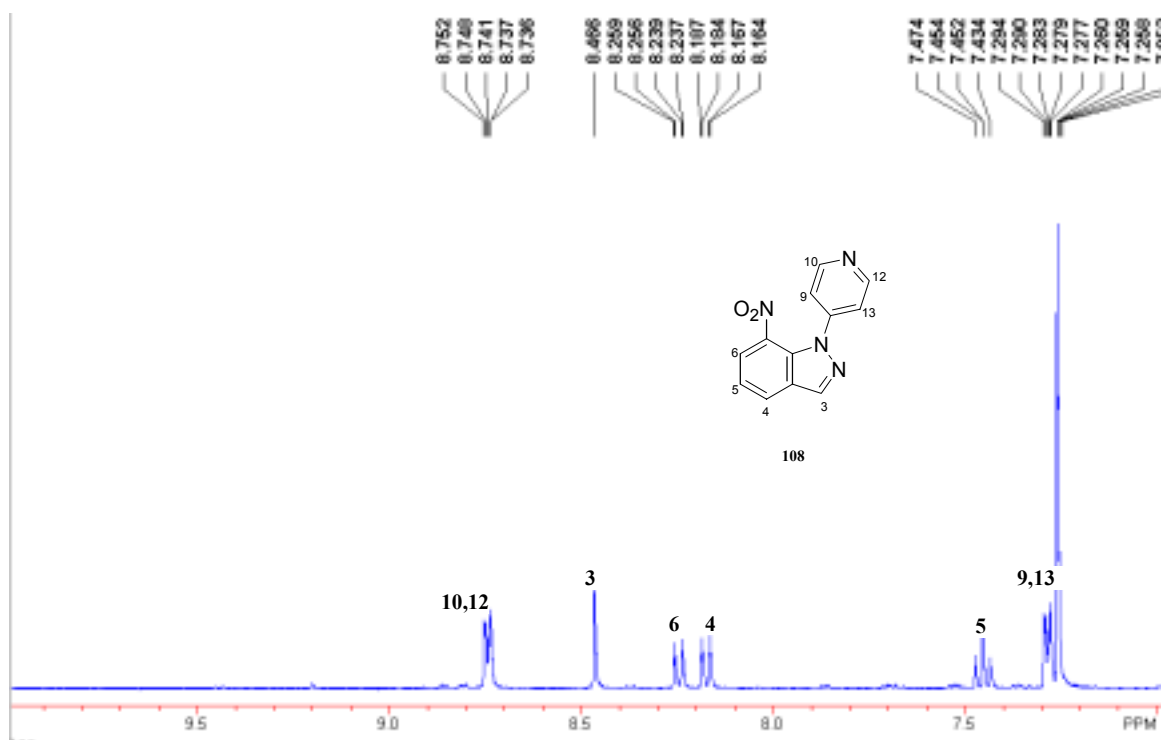
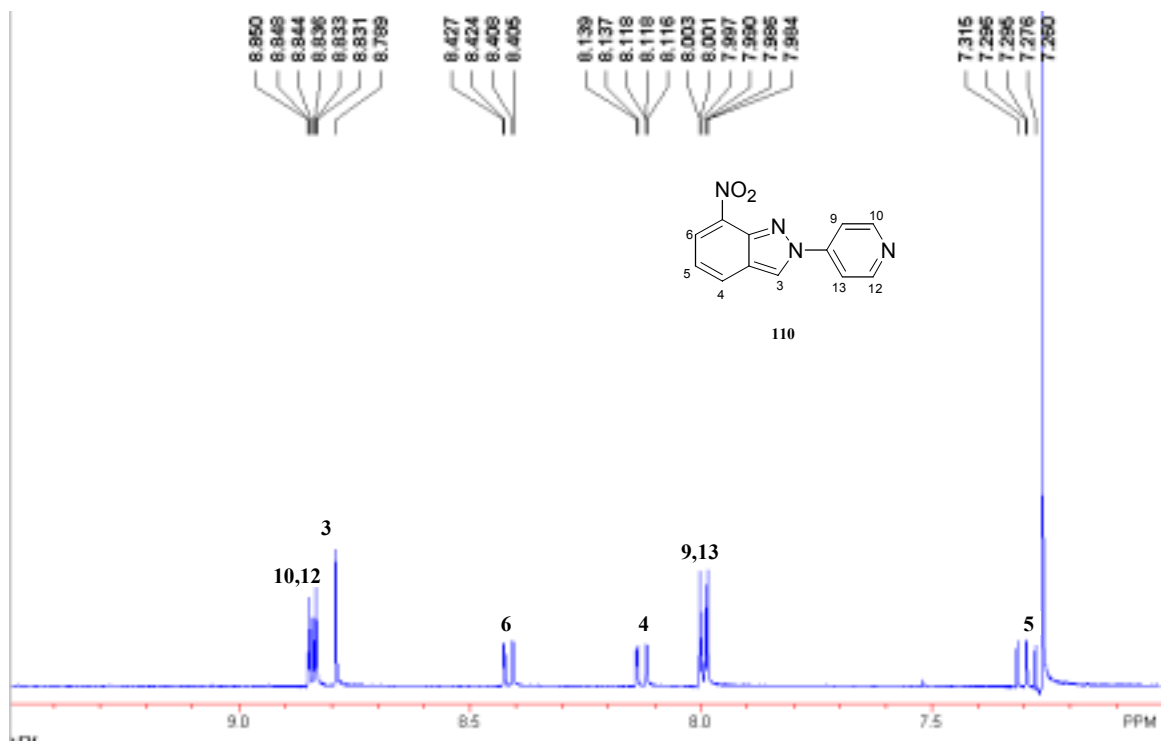


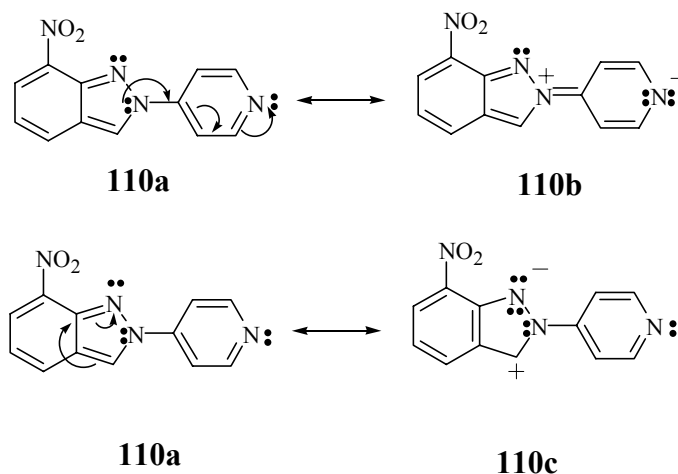
Figure 10.  $^1\text{H}$  NMR spectrum (instrument frequency = 400 MHz) of **108** in  $\text{CDCl}_3$ .



**Figure 11.** <sup>1</sup>H NMR spectrum of **110** in CDCl<sub>3</sub>.

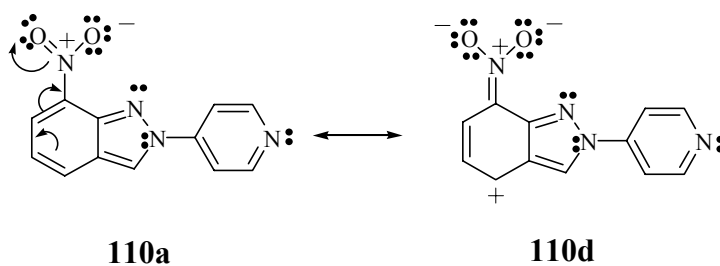
The signal assigned to the proton attached to C3 was shifted downfield in the *2H* isomer. Pyridine can act as an electron withdrawing group and decrease the electron density at C3 more effectively in **110** than **108** with the resonance contributor **110b** where neighbouring nitrogen N1 has a full positive charge and the resonance contributor **110c** where the electrons of the double bond localized on the N2 resulting a full positive charge on C3 as shown in Scheme 47. This is consistent with the downfield shift of the signal for the proton at C3.

**Scheme 47. Resonance structures responsible for the downfield shift of H3.**



The signal for the proton at C6 also was shifted 0.2 ppm downfield in the *2H* isomer. In addition to the electron withdrawing effect of the pyridinyl group, electron delocalization to the nitro group via resonance (**110d**) is favored for the *2H* isomer where the nitro group is co-planar with the benzene ring. The presence of the pyridinyl group at N1 (*1H* isomer) causes the nitro group to be twisted out of the plane, hence preventing the delocalization of electrons to the nitro group (Scheme 48).

**Scheme 48. Delocalization of electrons to the nitro group in the 1H isomer.**



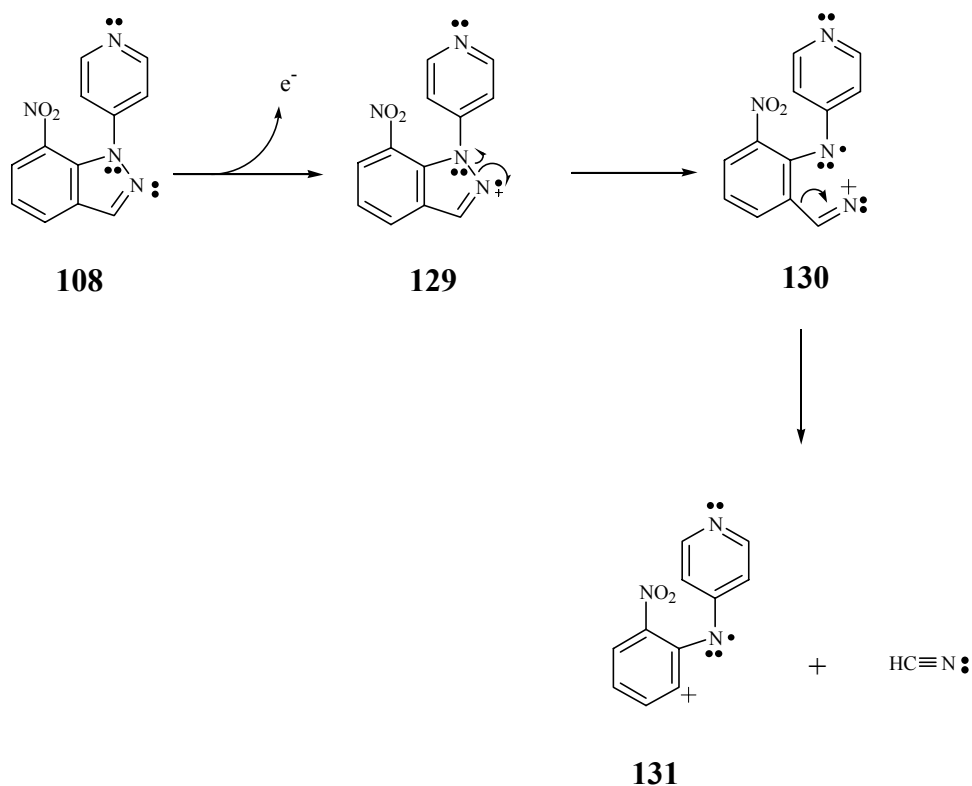
The signal for the protons at C9 and C13 in the *2H* isomer were shifted upfield due to the anisotropic effect of the nitro group. The electron cloud around oxygen shields these protons causing the signal to shift upfield.

Another interesting observation was the solvent effects on the chemical shifts of the signals, the most significant one being the signal assigned to the proton at C3. In the presence of DMSO-d<sub>6</sub>, the proton signal at C3 was shifted 0.9 ppm downfield when compared with the spectrum obtained in CDCl<sub>3</sub>.

#### 4.1.3.2. COMPARISON OF THE GC-EI MASS SPECTRA

As part of the characterization of the isomeric products we examined their GC-EIMS fragmentation patterns. Of particular interest were the two fragment ions at  $m/z = 223$  and  $m/z = 213$  which were present in only one of the two spectra. The  $M^+ - 27$  peak at  $m/z = 213$  corresponding to the loss of HCN (27 amu) was present only for the *1H* isomer. The loss of HCN from  $M^+$  of **108** can be explained as outlined in Scheme 49.

**Scheme 49. Loss of HCN from 108 results in the formation of the radical cation 131.**



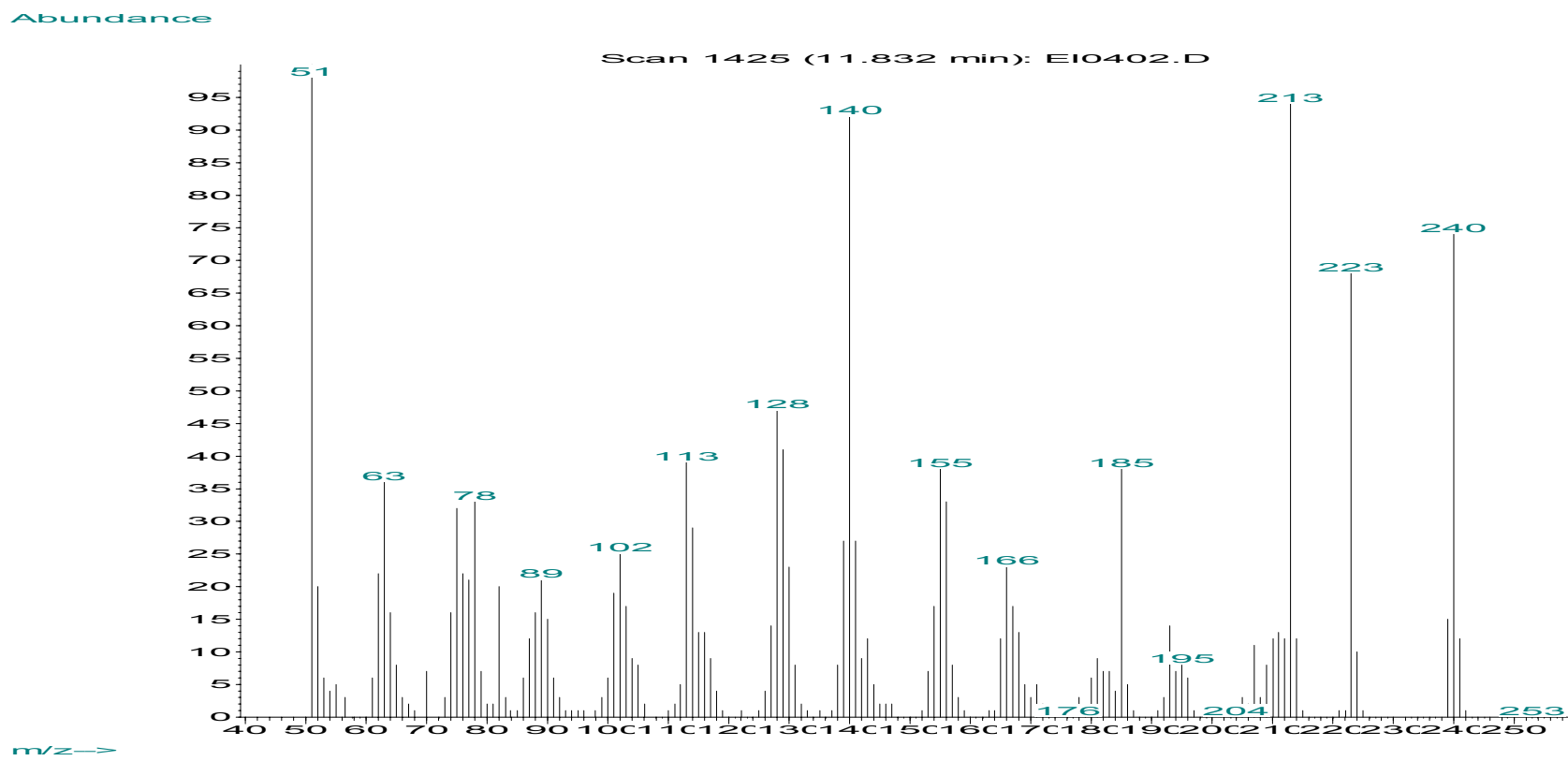


Figure 12. GC-EI mass spectrum of the compound 108.

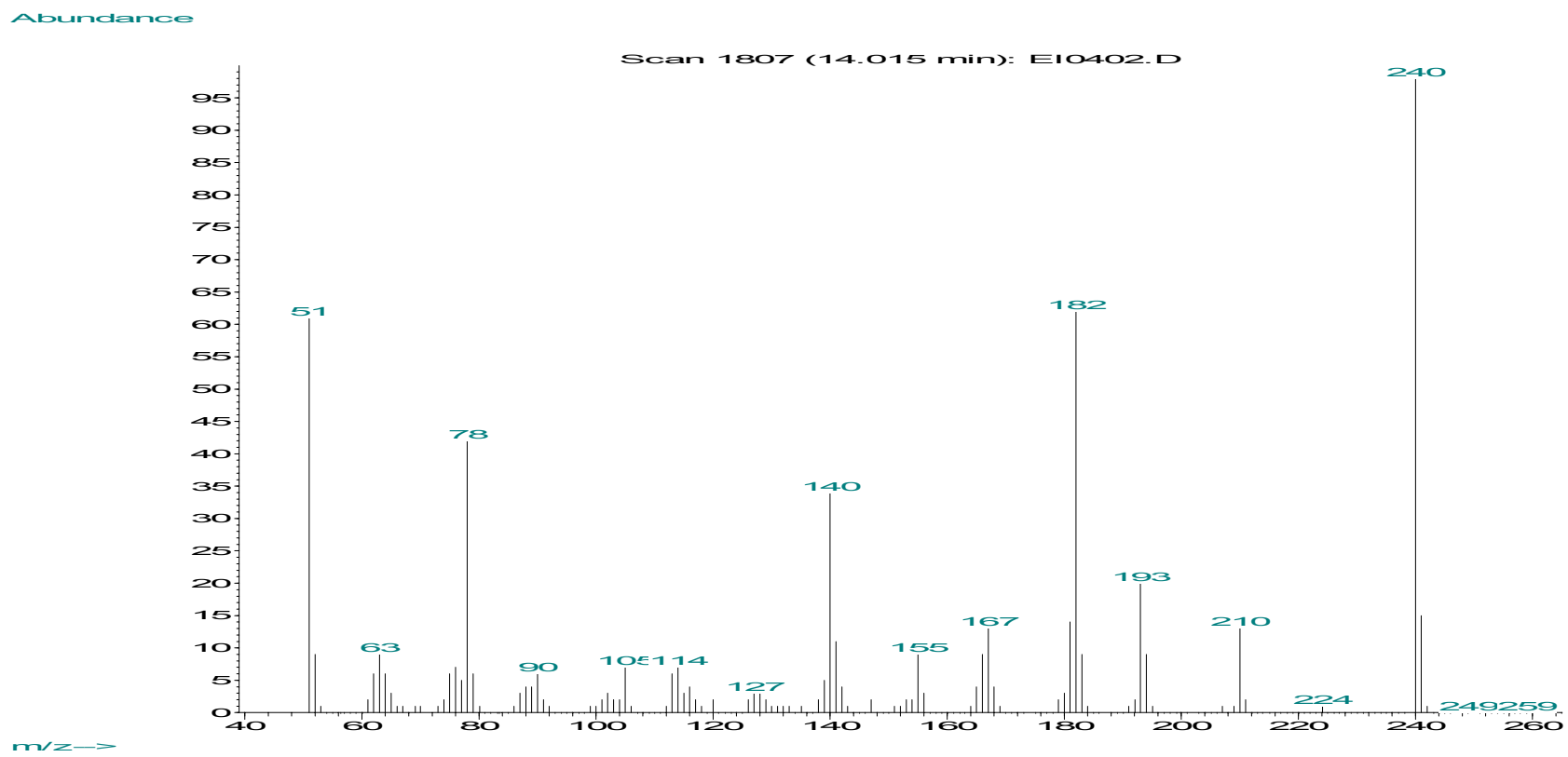
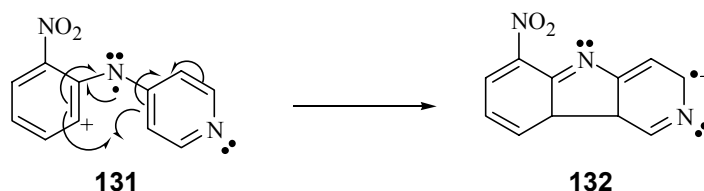


Figure 13. GC-EI mass spectrum of the compound 110.

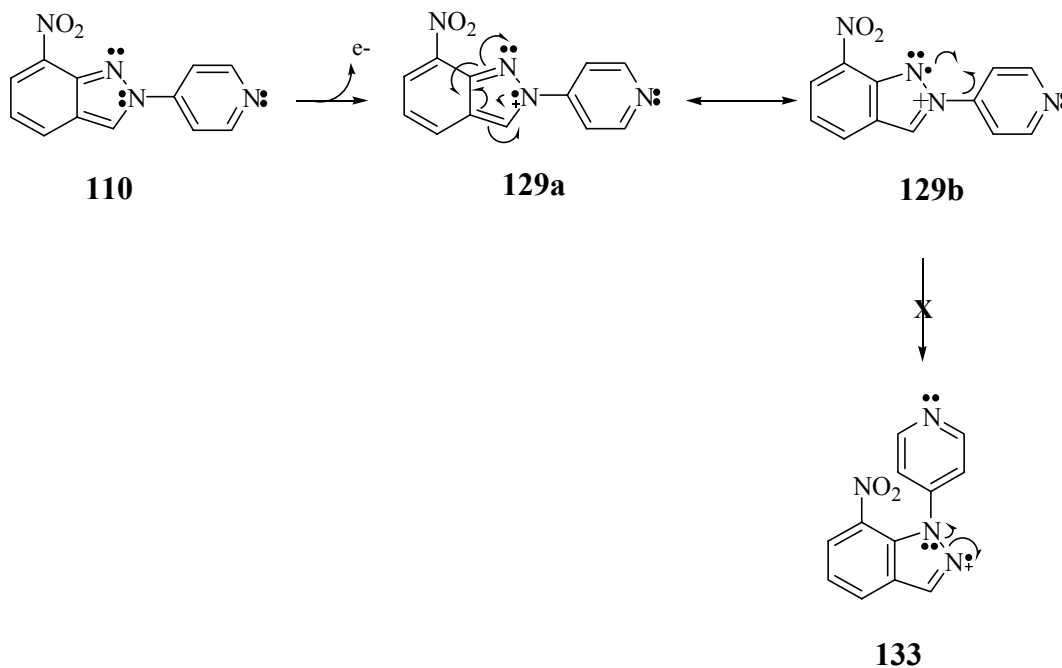
The radical cation **131** can be stabilized further via the formation of a 5-membered ring as shown in Scheme 50.

**Scheme 50. Suggested pathway for the stabilization of the radical cation (131) via the formation of a 5-membered ring.**



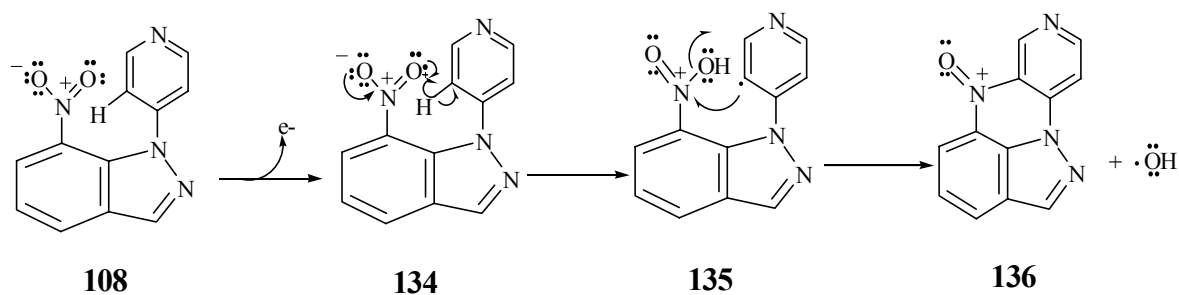
The loss of HCN from **110** requires the rearrangement of the radical cation **129** to **133** (Scheme 51) which is unlikely to take place due to the steric hindrance caused by the presence of the nitro group at C7. Therefore  $m/z = 213$  peak is observed only for the *1H* isomer.

**Scheme 51. Rearrangement of the pyridine group to allow the loss of HCN is not possible due to the steric hindrance of the nitro group in the 2H isomer.**



Another difference between the two spectra was the presence of an ion corresponding to the loss 17 amu from the parent ion. This loss may be attributed to the loss of  $\cdot\text{OH}$ . The following pathway is suggested to account for this fragmentation (Scheme 52). The proposed fragmentation is only possible for the *IH* isomer. The radical cation, formed after the loss of OH, can be stabilized via the concerted formation of a 6-membered ring **136**.

**Scheme 52. Suggested mechanism for the loss of OH begins with the H atom abstraction from the pyridine ring.  $\alpha$ -Cleavage gives the hydroxyl radical and the stabilized six-membered ring **136**.**



#### 4.1.4. INVESTIGATION OF THE REACTION MECHANISM

At this point we were able to assign unambiguously the regiochemistry of the previously obtained 4-(7-nitroindazolyl)pyridine as the *2H* isomer **110**. The previous tentative assignment, therefore, was incorrect. Also we detected and isolated the minor *1H* isomer **108** which had not been reported previously. However, the yield for the *1H* isomer was very low and enough material for complete characterization was not available. Therefore the next step was to attempt the preparation of the *1H* isomer **108**.

The first study towards this goal was the investigation of the reaction illustrated in Scheme 41 under different conditions using GC-EIMS to monitor the reaction progress. Unlike the previous experiments, this time the crude reaction mixture itself was analyzed by GC-EIMS instead of the ethyl acetate extracts. This was done in an attempt to show all of the components of the reaction mixture, whether or not they are soluble in ethyl acetate and, hence, to give more information on the course of the reaction.

The formation of the indazolyl anion may be a key step in the reaction pathway. Therefore we designed two experiments to verify the role of the base. The effect of the added base on the UV chromophore of 7-nitroindazole (**68**) was examined. A shift to higher wavelengths was observed when NaOH (excess) was used as the base showing the formation of the indazolyl anion. However, there was no significant shift when TMP (excess) was used as the base (Figure 14).

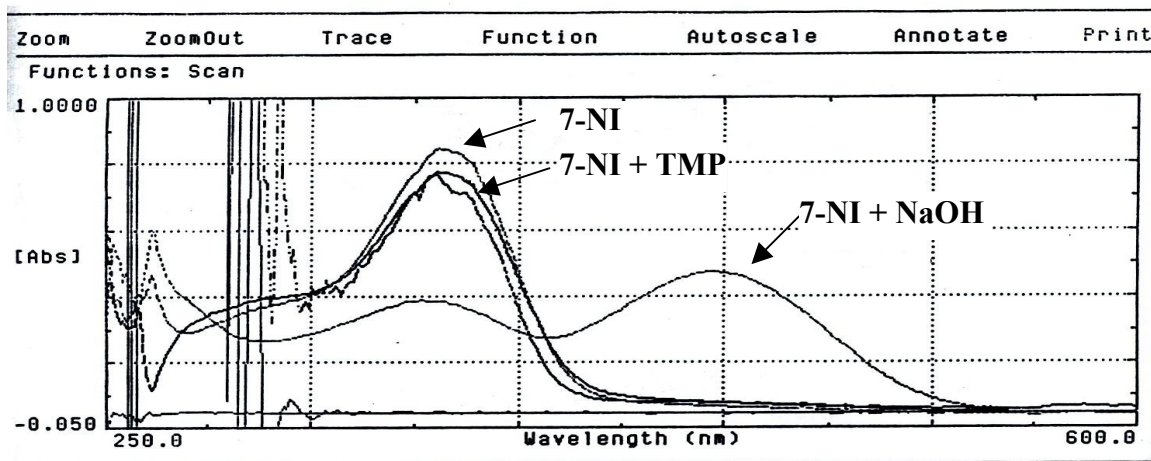


**Figure 14. UV spectrum of 7-NI in the absence of base, in the presence of TMP and in the presence of NaOH**

This raised the possibility that base was not required for this reaction. The coupling reaction was carried out without base and analyzed by GC-EIMS. The parent ion peak corresponding to the starting material 7-NI [**68** ( $m/z = 163$ )] did not decrease and TIC tracings did not show a peak corresponding to the product ( $m/z = 240$ ) even at high temperatures (100 °C) (Figure 15). This led to the conclusion that the base is essential for the product formation. Therefore, with 7-NI the indazolyl anion is a key intermediate in the reaction as shown in Scheme 53.

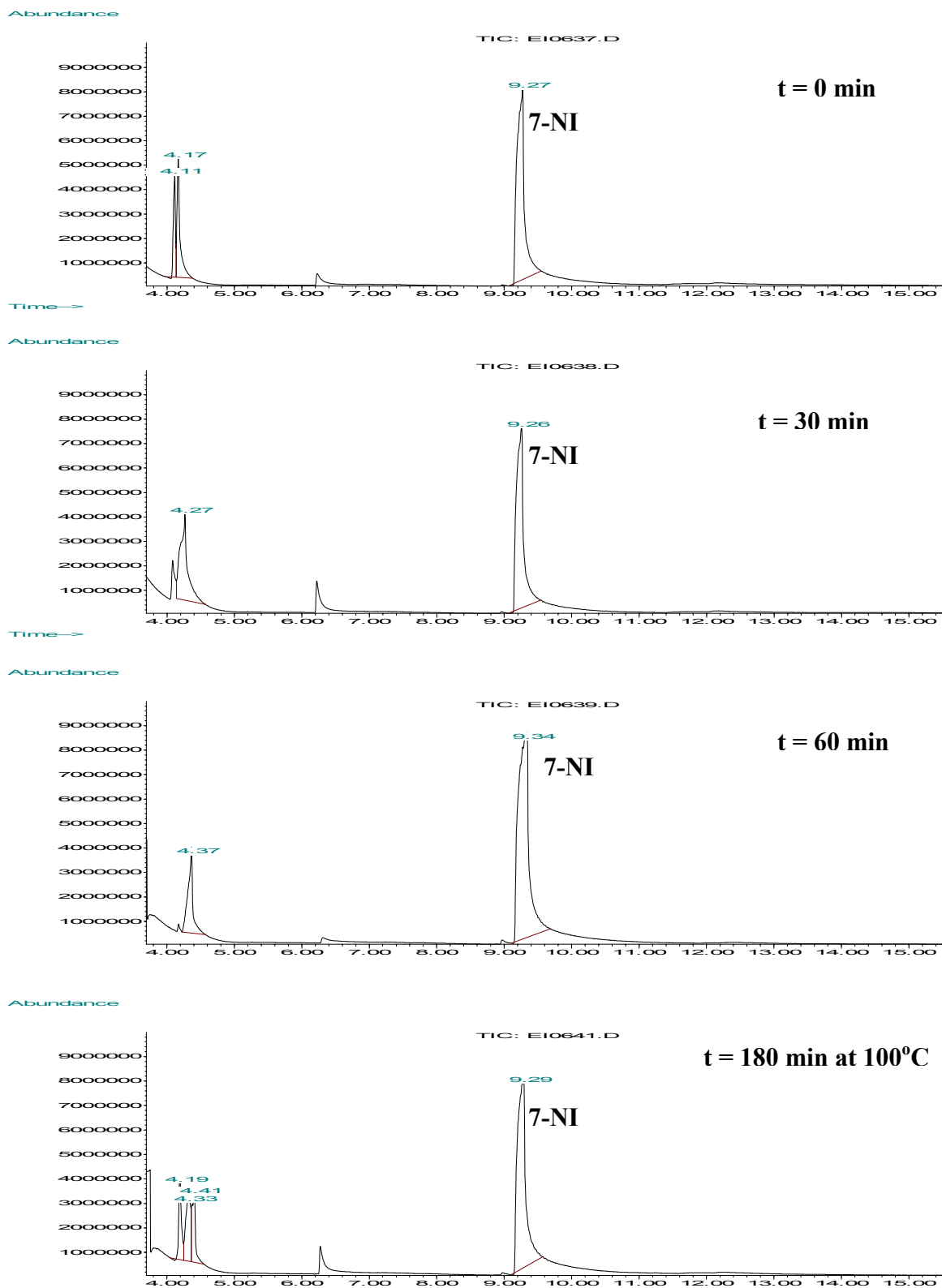
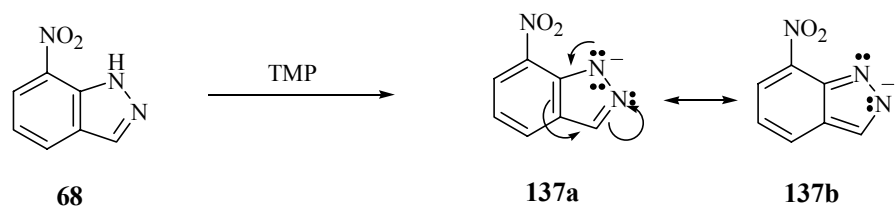


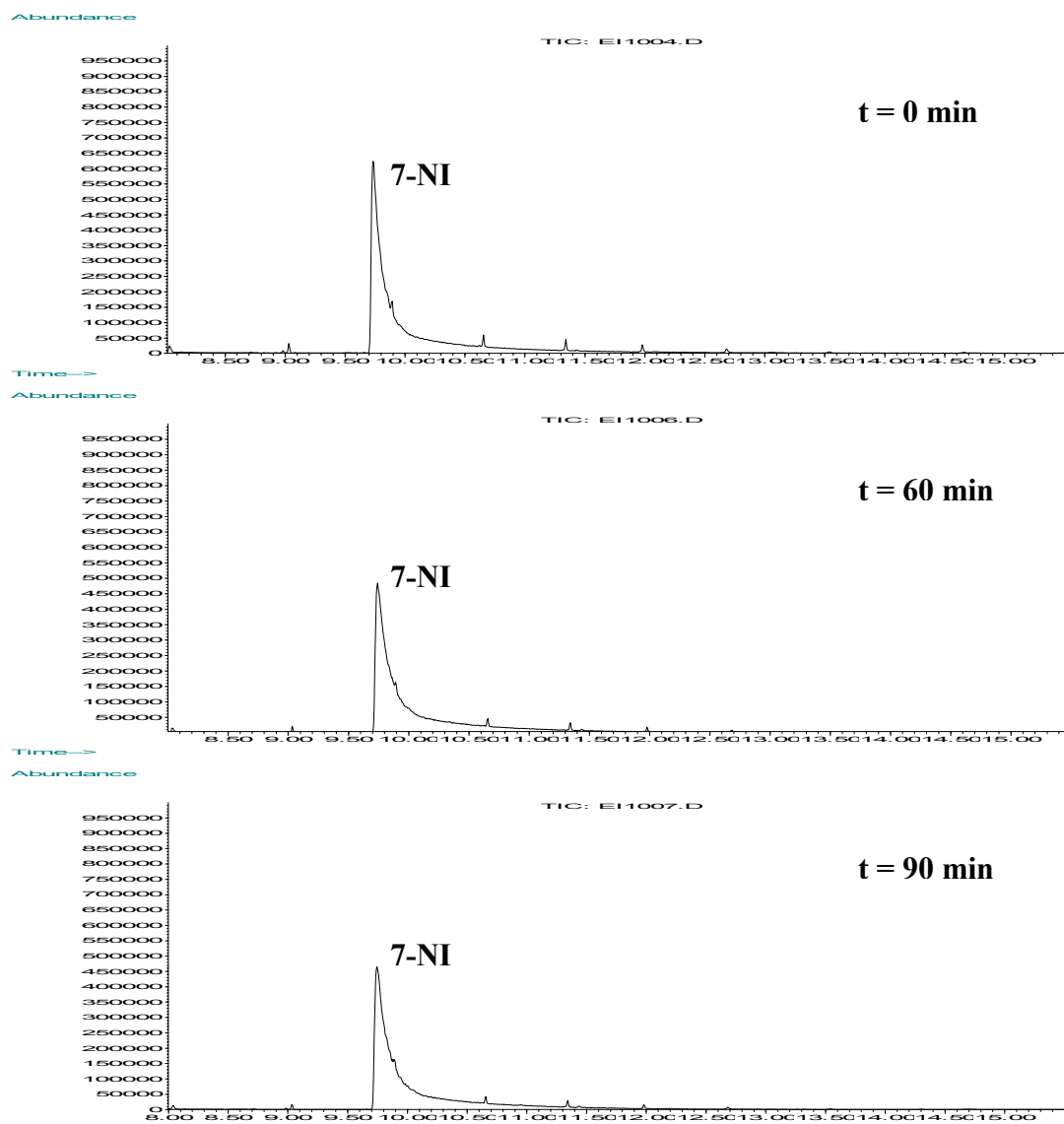
Figure 15. GC-EIMS TIC monitoring of the coupling reaction shown in Scheme 41.

Apparently TMP (it was chosen due to its suitability for GC-MS monitoring) forms only a small amount of the anion **137** (UV experiment) which nevertheless is sufficient to catalyze the reaction.

**Scheme 53. Abstraction of the imino hydrogen by the base leads to the indazolyl anion 137a which can be represented as another resonance form in which the negative charge is on N2 (137b)**

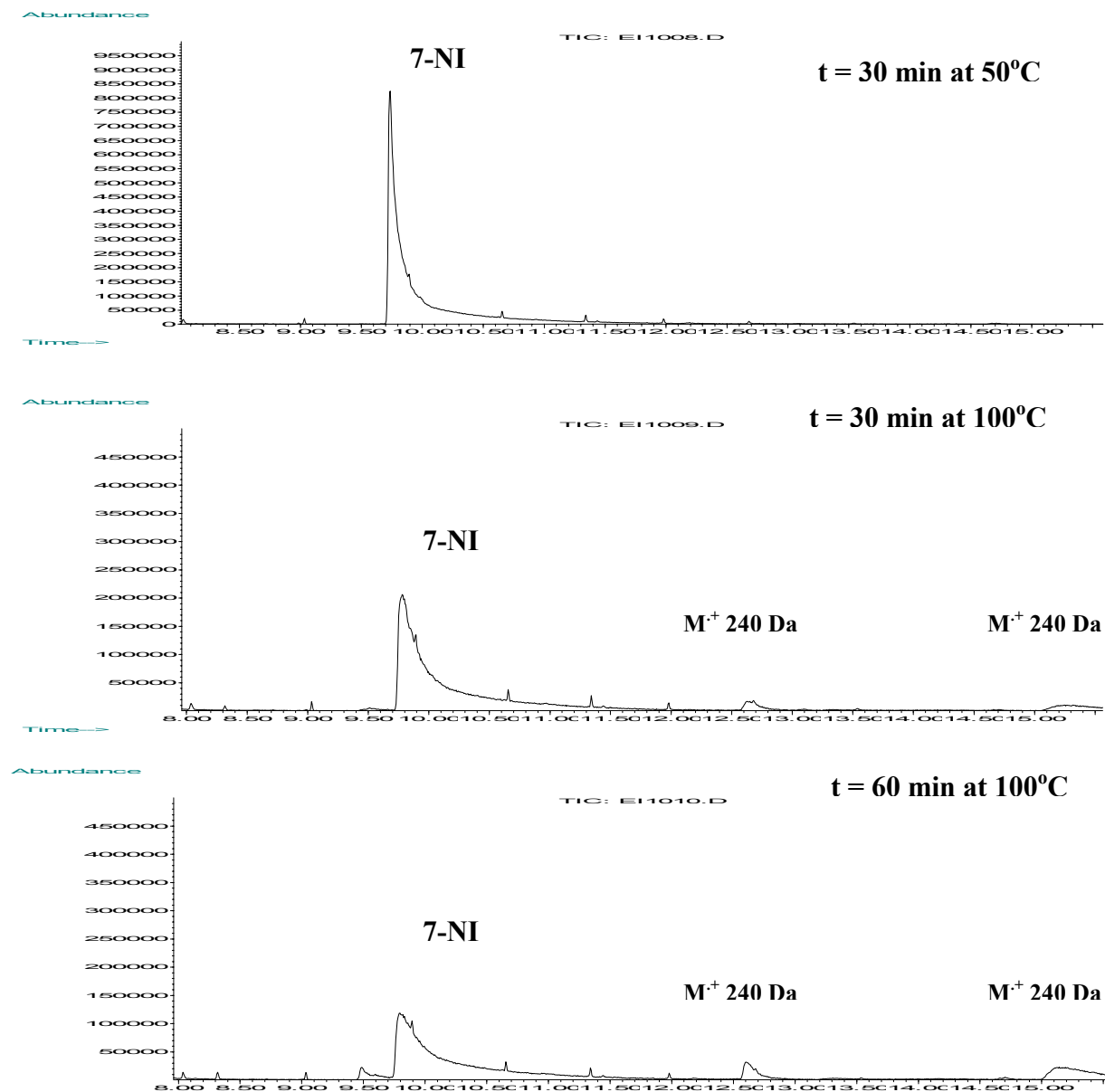


A second experiment was to monitor the reaction at various temperatures via GC-MS. Again the crude reaction mixture was diluted in MeOH and subjected to GC-MS analysis. There was no change in the composition of the reaction mixture at room temperature (Figure 16).



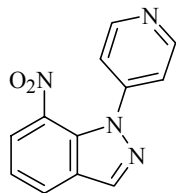
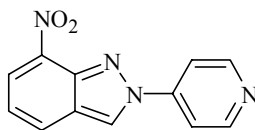
**Figure 16. GC-EIMS TIC monitoring of the coupling reaction shown in Scheme 41 at room temperature.**

After heating to 100 °C, a decrease in the peak corresponding to the starting material and the appearance of two new, weak peaks with retention times 12.6 and 15.1 minutes, was observed (Figure 17).



**Figure 17. GC-EIMS TIC monitoring of the coupling reaction shown in Scheme 41 at elevated temperatures.**

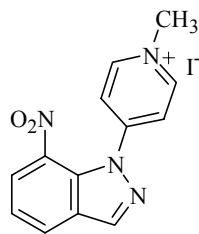
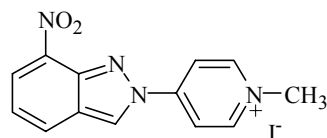
Both of these peaks displayed  $M^+$  at 240 Da and the retention times coincided with the expected retention times of **108** and **110**. The mass spectra of these ions matched with the mass spectra obtained previously for **108** and **110**.

**108****110**

After 30 minutes there was no significant increase in the intensity of the product peaks suggesting that the reaction stops after a certain period of time. The TIC tracing was complex but ions corresponding to 7-NI ( $M^+$  163), 4-chloropyridine ( $M^+$  113/115) and TMP ( $M^+$  141) were present. Addition of excess base or excess 4-chloro-1-methylpyridinium iodide did not re-initiate the product formation. This was already expected since both compounds were shown to be present in the reaction mixture.

At this point, it was not possible to explain why the reaction appeared to stop after a certain time. Particularly problematic was the observation that both reactants were still present in sufficient quantities to expect further reaction. This led us to explore an alternative way to monitor the progress of the reaction.

The GC-EIMS TIC tracings for the crude reaction mixtures were very complex with several unidentified peaks. Since the methylated products (**119** or **120**) are expected to lose the methyl group to form **108** or **110**, respectively, in the injection port, it was not possible to distinguish **119** from **108** or **120** from **110**. At this point monitoring the reaction by HPLC was considered.

**119****120**

The HPLC retention times of the starting materials were determined with standard solutions. We also injected a standard solution of the desmethyl compound **110** since it was the expected product based on previous experiments (Figure 18).

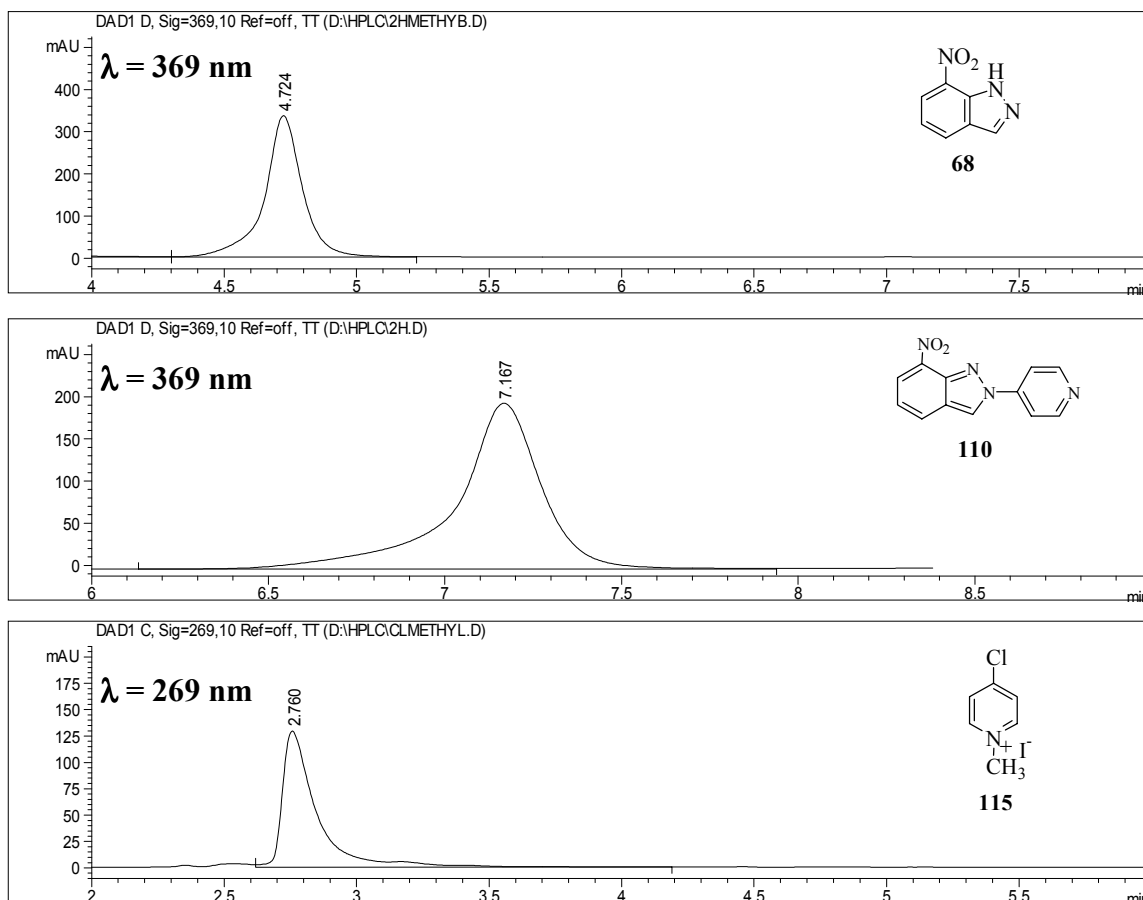


**Figure 18. HPLC tracings for the standard solutions of 68, 110 and 115.**

The reaction was run at 0.1 M concentration of the starting materials at room temperature. A mixture of 7-NI (1 equivalent), TMP (1 equivalent), and 4-chloro-1-methylpyridinium iodide [**115** (1 equivalent)] was prepared in DMF. The reaction mixture was monitored each 15 minutes by diluting a 10  $\mu$ L sample in 0.5 mL of the mobile phase (50% HCN 50% pH=4.7 buffer solution) and injecting onto the HPLC. After 15 minutes, the peak corresponding to 7-NI (4.8 min.) decreased and a new peak was observed with a retention time of 3.4 minutes (Figure 19).

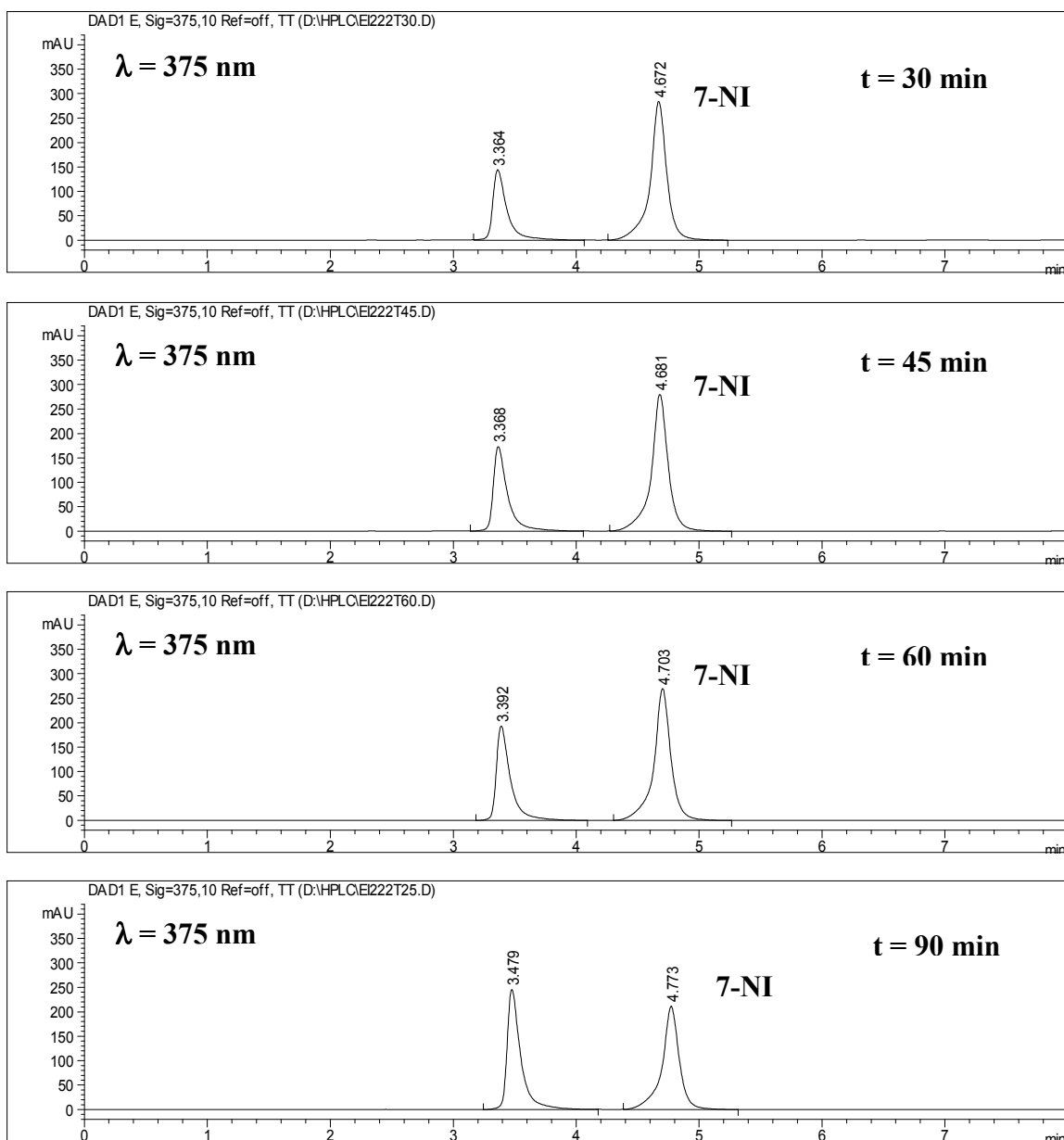
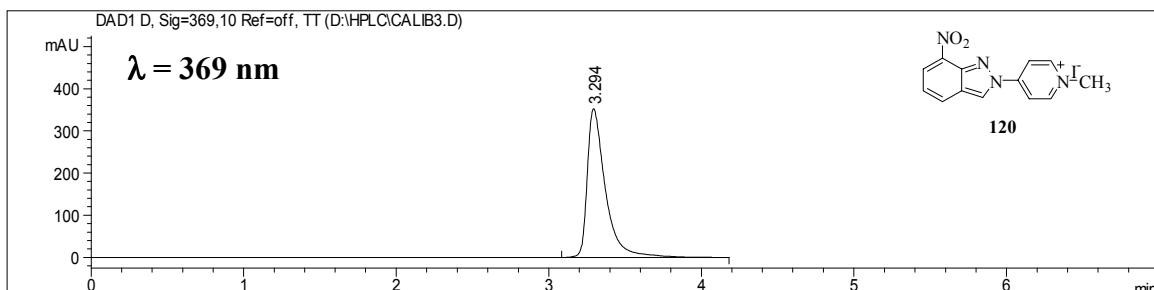


**Figure 19. HPLC tracings for the coupling reaction at room temperature.**

The intensity of the peak at 3.4 minutes kept increasing and the intensities of the peaks corresponding to both starting materials **68** and **115** (**115** was monitored separately at  $\lambda = 269$  nm) decreased. A precipitate began to form after 30 minutes.

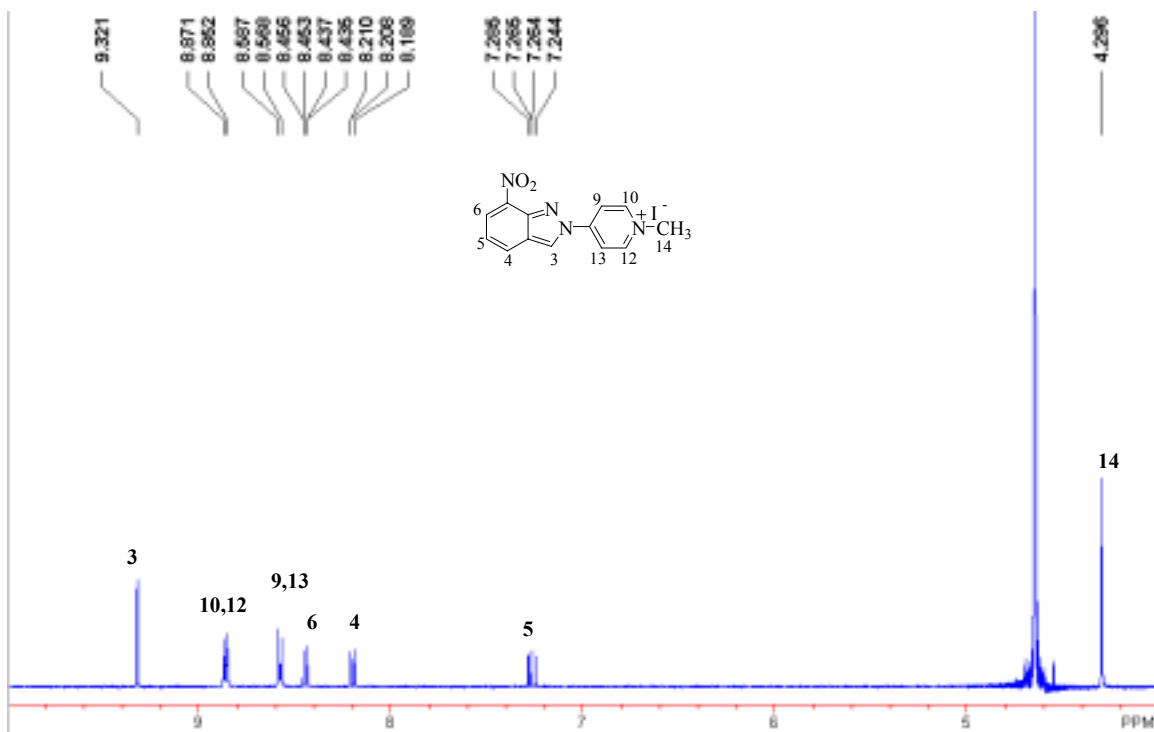
The retention time for the product was not the same as the demethylated compounds **108** or **110**. Therefore a standard solution of the pyridinium compound [(**120**) that had been prepared previously via methylation of **110**] was analyzed. It gave a

retention time of 3.3 minutes suggesting that **120** was likely to be the product of the reaction (Figure 20).



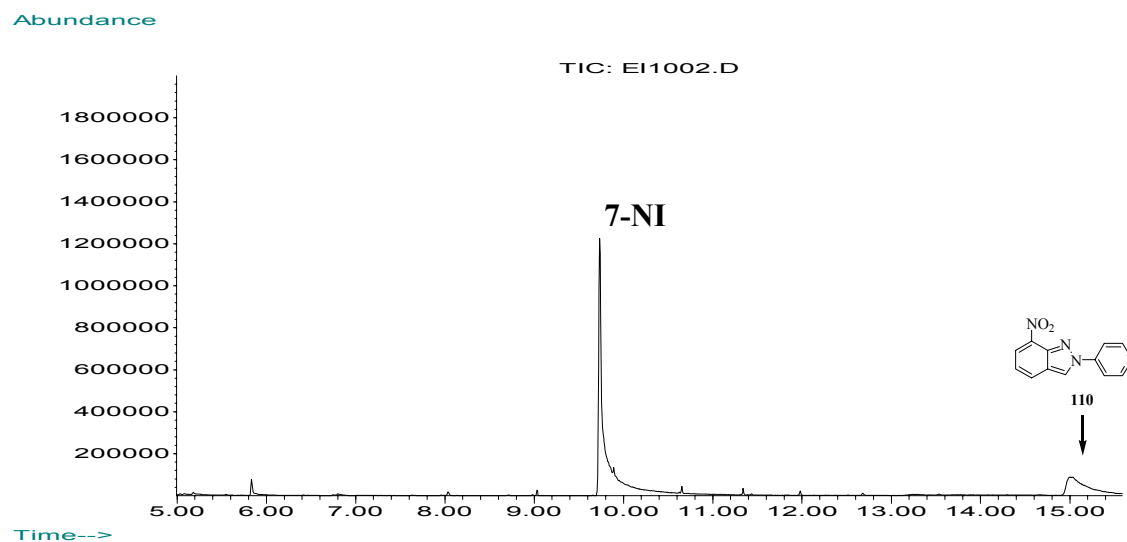
**Figure 20.** HPLC analysis of **120**.

The reaction was carried out on a larger scale. After 24 hours, the precipitate was collected. It was insoluble in ethyl acetate. The compound was re-crystallized from hot MeOH to give a 58 % yield. The  $^1\text{H}$  NMR spectrum for the compound established that it was indeed the methylated product **120** (Figure 21).



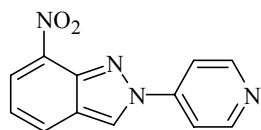
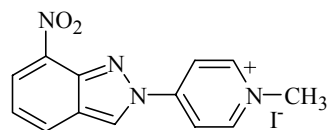
**Figure 21.**  $^1\text{H}$  NMR spectrum (instrument frequency=400 MHz) of **120** in  $\text{DMSO-d}_6$ .

Initially this finding seemed contradictory to the results obtained by GC-EIMS. Parallel GC-EIMS analyses performed in this experiment indicated that there was no product formation at room temperature. The product was forming only at elevated temperatures. However, HPLC analysis showed the rapid formation of **120** even at room temperature. In order to explain this behavior, compound **120** were analyzed by GC-EIMS. The TIC tracing shown in Figure 22 was obtained..



**Figure 22. GC-MS analysis of 120.**

It was obvious that the product of the room temperature chemistry **120** was decomposing under GC-EIMS conditions to form the starting material 7-NI and only a very small amount of **110**. Therefore, it was not possible to observe the product formation of the room temperature chemistry by GC-EIMS. It appeared that the reaction was not proceeding at room temperature. However, at high temperature, the demethylation was occurring in the reaction mixture to yield the demethylated product **110**. This demethylated product was stable under GC-EIMS conditions. This observation explains the earlier, incorrect conclusion that product formation was only possible at high temperatures.

**110****120**

Although we obtained only the *2H* isomer (**120**) at room temperature, it was possible to obtain a small amount of the demethylated *1H* isomer at elevated temperatures. Also the thermal production of 7-NI from pure **120** suggested that, at high temperatures it was possible, the reaction is reversible. Perhaps under the equilibrium conditions some of the slightly more stable *1H* isomer may be present and could account for the conversion of the *2H* isomer to the *1H* isomer obtained as the demethylated product **108**. Compound **120** was dissolved in DMF and heated to 100 °C in the presence and absence of TMP as the base. The reaction mixtures were analyzed by HPLC. No change was observed in the absence of base even at high temperatures. However, in the presence of base, the intensity of the peak corresponding to **120** decreased and a peak with a retention time identical to 7-NI began to appear (Figure 23).

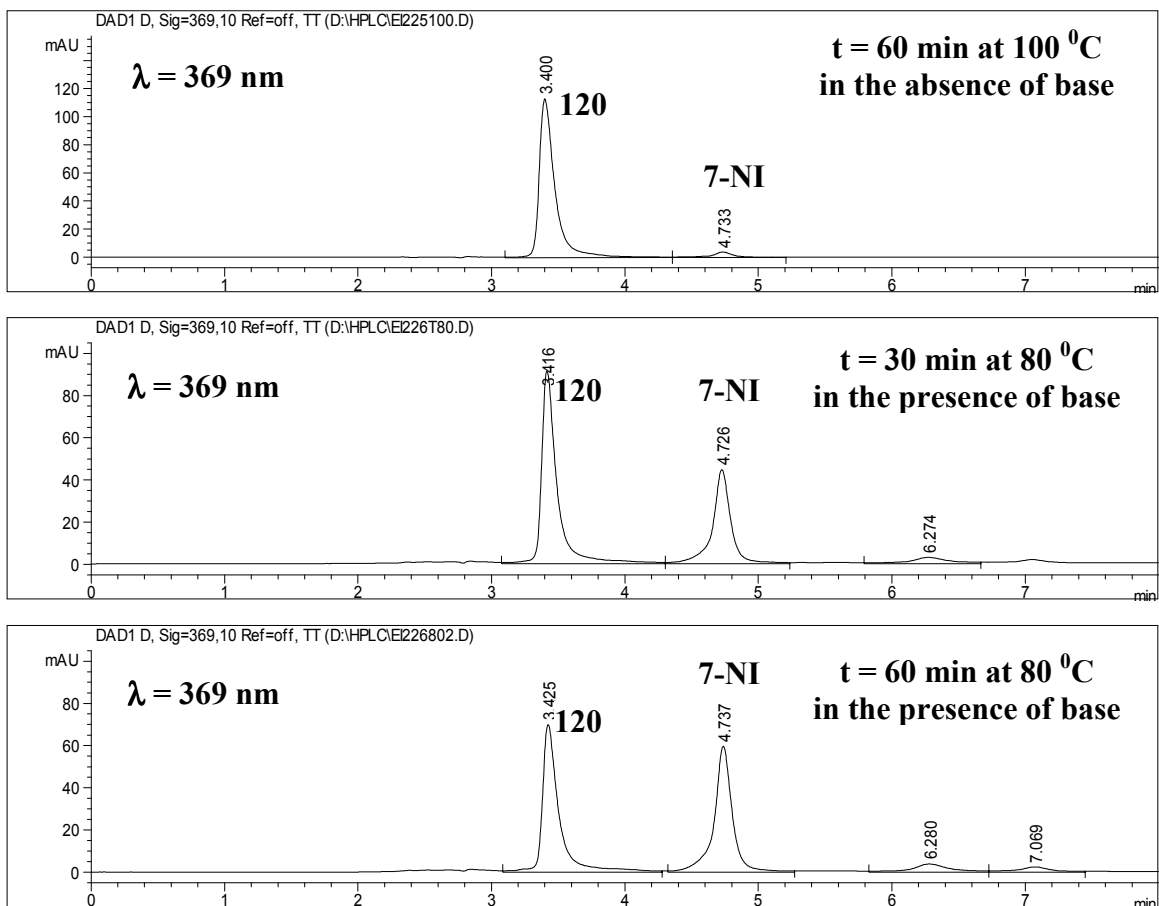


**Figure 23. HPLC tracings for the decomposition of 120 in the presence of TMP.**

Another peak at 3.16 minutes increased with time but was observed only at 269 nm (Figure 24). We tentatively assigned this peak to be due to the 4-iodo-1-methylpyridinium species **121**.

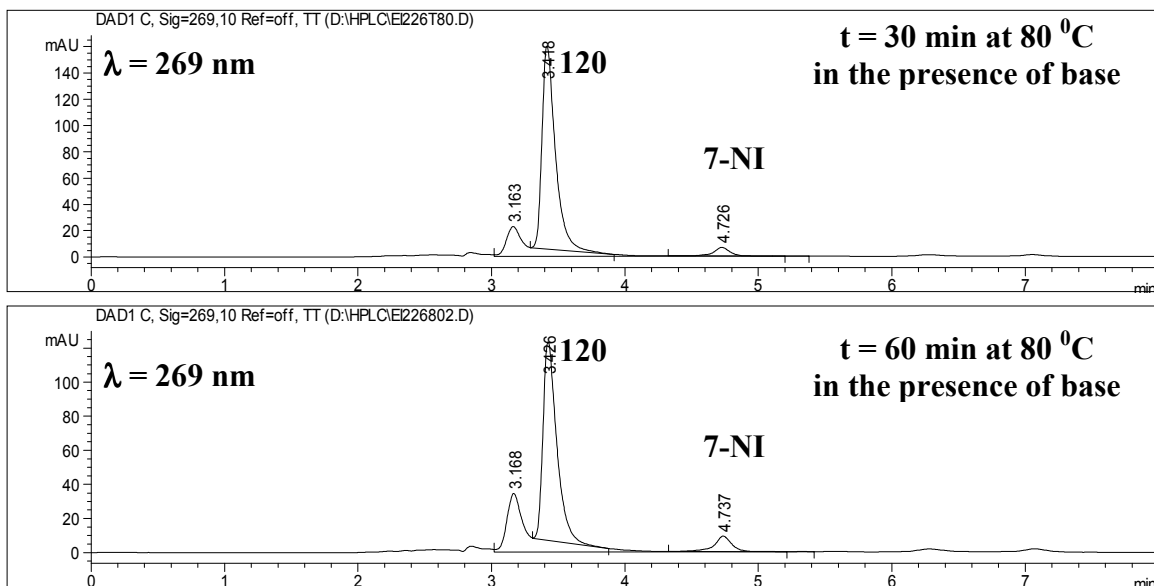
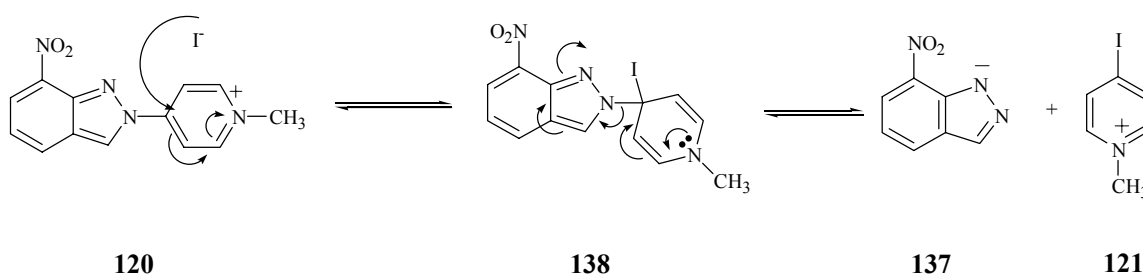


**Figure 24.** HPLC tracings for the decomposition of **120** in the presence of TMP at **269 nm**.

The following mechanism is proposed to account for the loss of the starting material (Scheme 54):

**Scheme 54.** After the formation of the intermediate **138** at high temperatures equilibrium shifts to the right forming 7-nitroindazolyl anion (**137**) and **121**.



According to this mechanism, **120** was decomposing to give the 7-nitroindazolyl anion and the 4-iodo-1-methylpyridinium species **121**, the peak seen at 3.16 minutes in the HPLC tracings at 269 nm (Figure 24). After work-up, the 7-nitroindazolyl anion is converted to 7-nitroindazole (**68**). However, it was not possible to explain the function of base by the above mechanism. At this point, the reaction is still reversible. We suggest

that an irreversible sequence may involve the demethylation of **121** to form 4-iodopyridine and methyl iodide. Then the methyl iodide is trapped by the TMP to give the N-methyl-TMP product **140** which can not be detected by HPLC-DA due to the lack of a chromophore (Scheme 55).

Therefore, we re-examined the GC-EIMS TIC tracings in an attempt to detect **140**. There was one major peak of interest at 6.03 minutes with  $M^+$  155 Da which corresponds to **140** (Figure 25). The fragmentation pattern was similar to that of TMP following the loss of a 15 amu fragment, which is likely to be the N-methyl group. The GC-EIMS analysis of the synthetic **140** gave an identical retention time and a mass spectrum confirming this assignment. This is consistent with the proposal that **121** undergoes demethylation to form 4-iodopyridine (**139**). Then, TMP reacts with the methyl iodide which is the irreversible step in the overall sequence (Scheme 55).

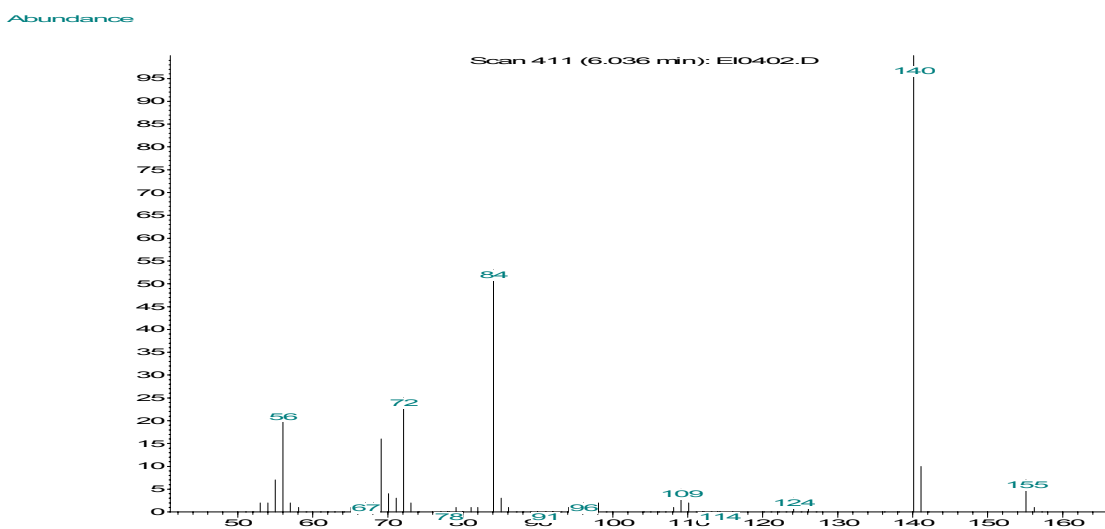
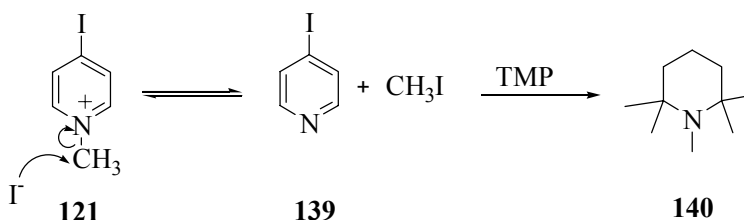


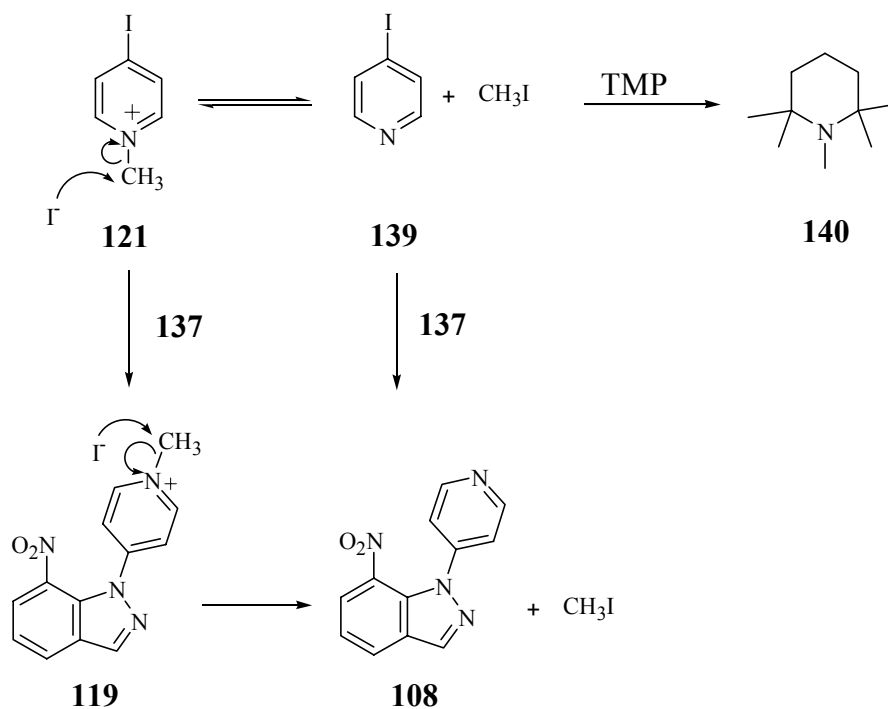
**Figure 25.** GC-EIMS spectrum of the peak thought to be a TMP adduct.

**Scheme 55.** Demethylation of **121** to give 4-iodopyridine (**139**) was yielding methyl iodide which would be trapped by TMP to make the reaction irreversible.



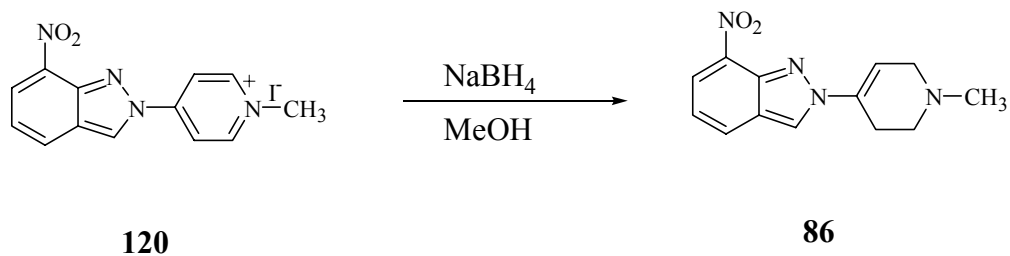
This also explains the formation of the *IH* isomer **108** with low yield at high temperatures. Under vigorous reaction conditions **139** could react with the indazolyl anion to form the slightly more stable *IH* isomer **108** or reaction of **121** with indazolyl anion followed by demethylation could result in the formation of **108** (Scheme 56). However, the steric hindrance caused by the nitro group makes this reaction unfavorable.

**Scheme 56.** After the demethylation step **139** could react with **137** under vigorous reaction conditions to form **108**.



As the final step in our synthetic pathway to the “prodrug” of 7-NI **120** was the reduction of **120** to the corresponding tetrahydropyridine **86** as shown in Scheme 57.

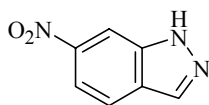
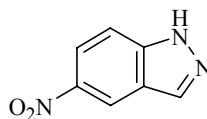
**Scheme 57.** Reduction of the pyridinium compound **120** to the corresponding tetrahydropyridine **86**.



**4.2. SYNTHESIS OF TWO STRUCTURALLY RELATED COMPOUNDS  
THE *1H* AND THE *2H* ISOMERS OF 1-METHYL-4-(6-NITROINDAZOLYL)-  
1,2,3,6-TETRAHYDROPYRIDINES (141 AND 142) AND 1-METHYL-4-(5-  
NITROINDAZOLYL)-1,2,3,6-  
TETRAHYDROPYRIDINES (143 and 144)**

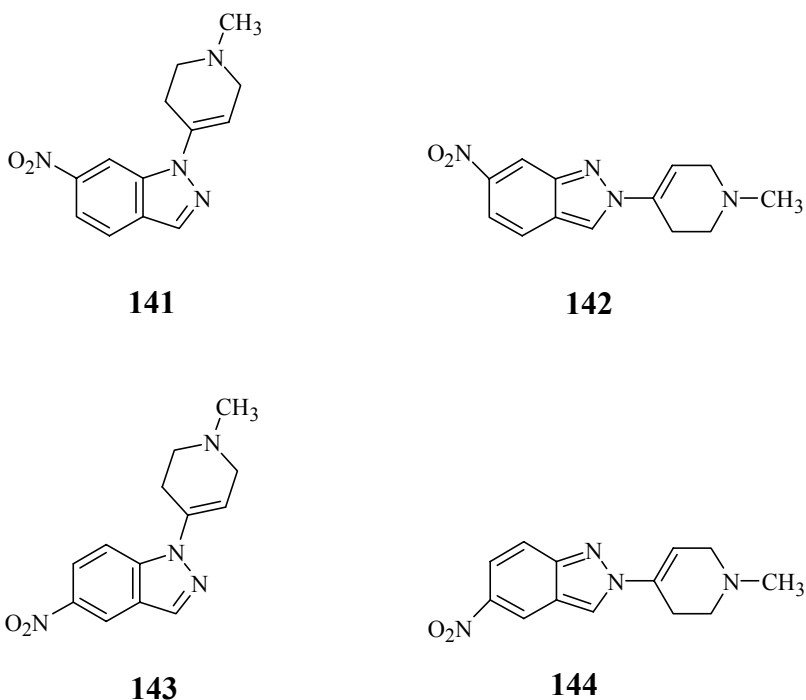
Our success in the coupling reaction between 4-chloro-1-methylpyridinium iodide (**115**) and 7-NI (**68**) led us to extend our studies to two structurally similar compounds 6-NI (**122**) and 5-NI (**123**), and to apply this reaction as a general method to obtain “prodrugs” of these compounds.

Babbedge *et al.* reported that two positional isomers of 7-nitroindazole, 6-nitroindazole (**122**) and 5-nitroindazole (**123**), like 7-nitroindazole (**68**), also inhibit rat cerebellar NOS.<sup>173</sup> However, 6-NI and 5-NI were 35 (IC<sub>50</sub> = 31.6 μM) and 55 (IC<sub>50</sub> = 47.3 μM) times less potent than 7-NI, respectively, which has an IC<sub>50</sub> value of 0.9 μM.

**122****123**

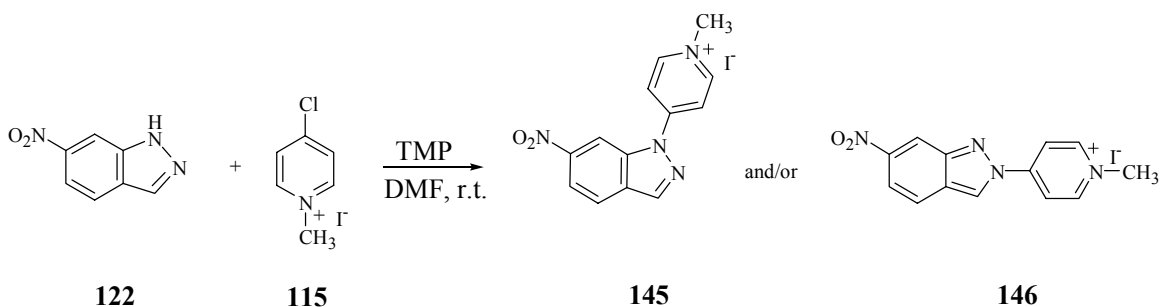
Our interest in **122** and **123** is due to several reasons. If these compounds are more potent MAO-B inhibitors than 7-NI, comparison of their neuroprotective effects with the neuroprotective effect of 7-NI may give information on the involvement of MAO-B versus nNOS inhibition in neuroprotection. If inhibitors of MAO-B, these structures could prove useful in structure activity relationship (SAR) studies directed to defining the active site of this enzyme. Finally, synthesis of potential “prodrugs” **141/142** of **122** and **143/144** of **123** may provide information on the synthetic pathway which may help us achieve the synthesis of *1H* prodrug **86** of 7-NI.

<sup>173</sup> Babbedge, R.C., Bland-Ward, P.A., Hart, S.L., Moore, P.K. (1993) Inhibition of rat cerebellar nitric oxide synthase by 7-nitroindazole and related substituted indazoles. *Br. J. Pharmacol.* **110**, 225-228



The same pathway as that used for the synthesis of 1-methyl-4-(7-nitroindazol-2-yl)pyridinium iodide (**120**) was pursued (Scheme 58).

**Scheme 58. Nucleophilic aromatic substitution reaction between 6-nitroindazolyl anion and 4-chloro-1-methylpyridinium iodide (**115**).**



The reaction was monitored by HPLC. After 5 minutes the reaction mixture turned cloudy and a solid began to separate from the reaction mixture. After 30 minutes the peak corresponding to 6-NI (5.0 minutes) had almost completely disappeared and two new peaks had appeared at 3.0 minutes and 3.1 minutes. These are likely to be the two possible isomers **145** and **146** (Figure 26).

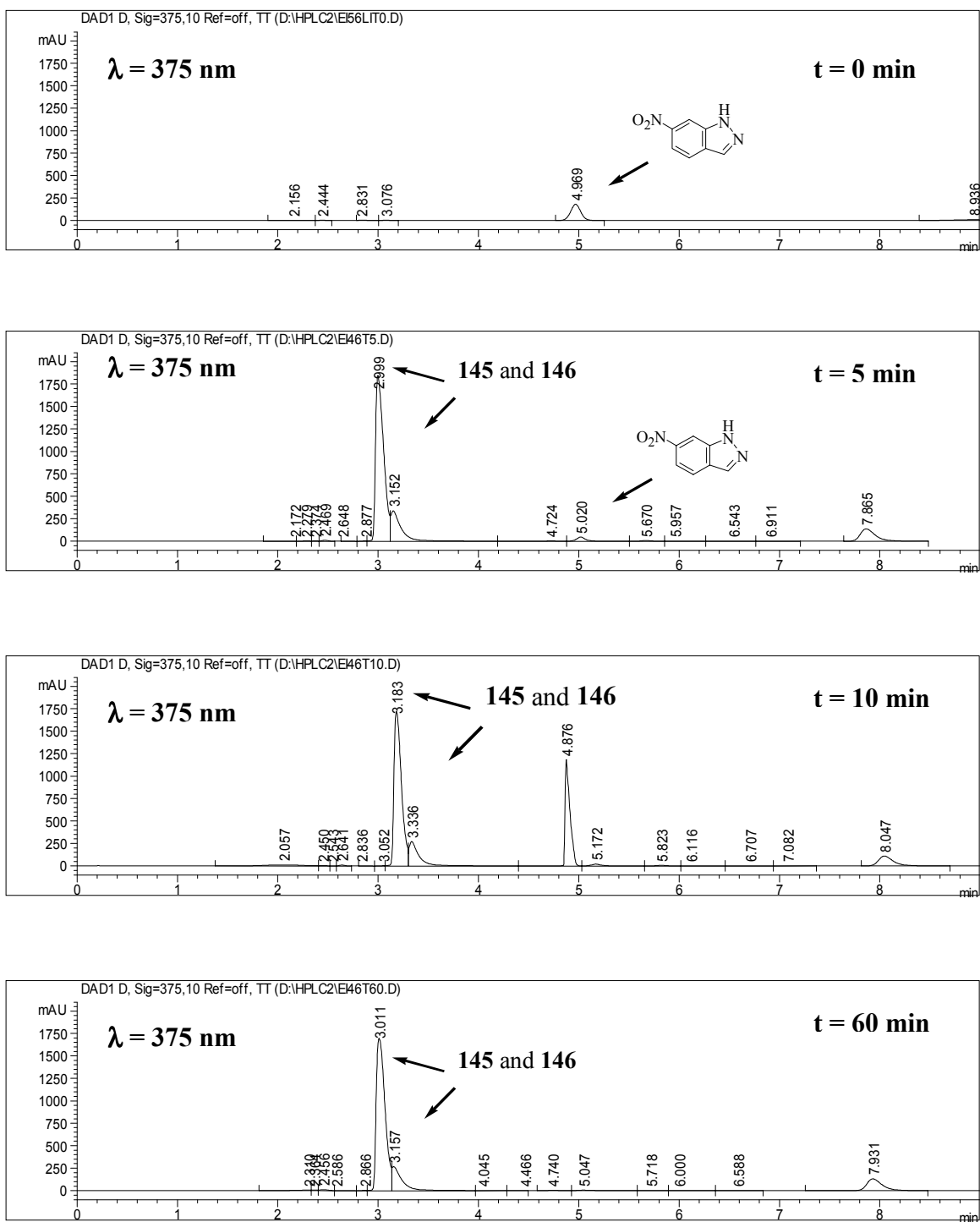


**Figure 26. HPLC monitoring of the reaction shown in Scheme 58.**

In addition to the increasing intensities of the product peaks, another peak with a retention time of 4.8 minutes was seen in HPLC tracings during the course of the

reaction. This peak, however, eventually disappeared. Perhaps this transient intermediate is the initial tetrahedral adduct (see below) formed during the course of the reaction.

The solid that separated from the reaction mixture was filtered and was crystallized from hot methanol/water to give product in 85 % yield. The  $^1\text{H}$  NMR spectrum (Figure 27) confirmed the presence of exclusively one compound that could be assigned to **145** or the regioisomer **146**. The isolation of the minor isomer, which remained in solution, was not attempted.

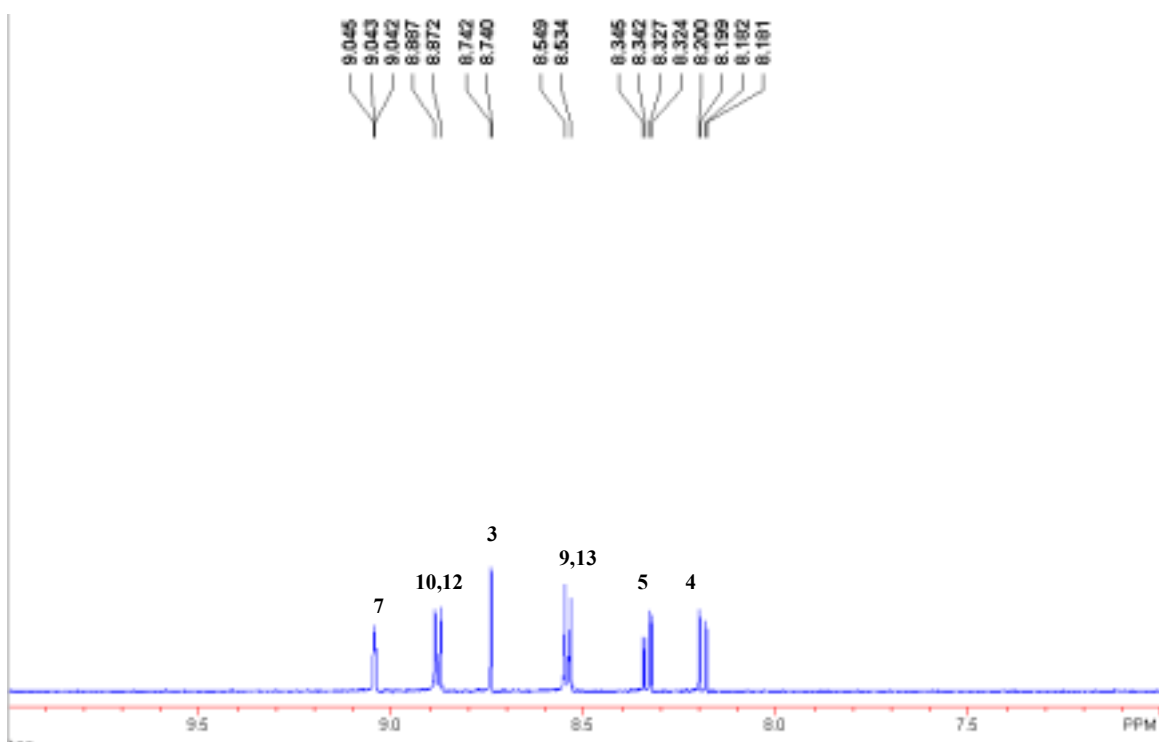
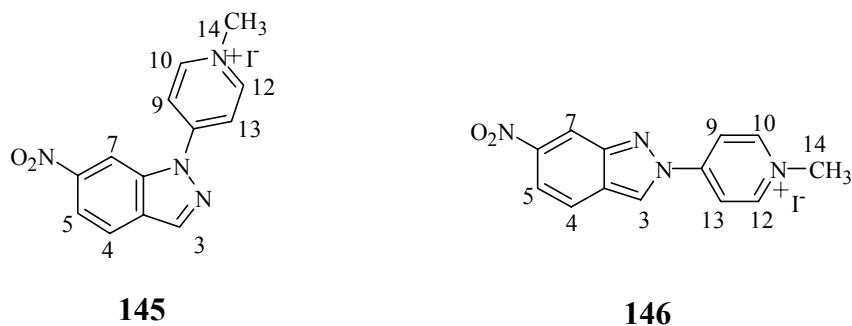
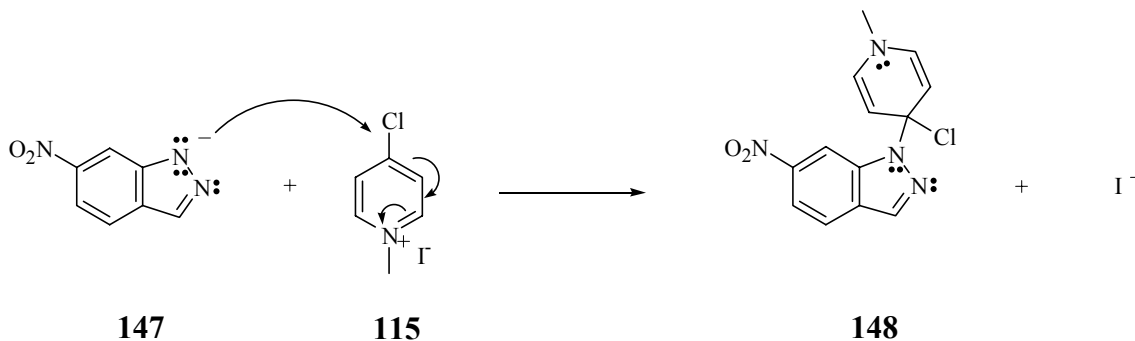


Figure 27.  $^1\text{H}$  NMR spectrum (instrument frequency = 500 MHz) of the product **145** or **146** in  $\text{D}_2\text{O}$ .

In order to determine the regiochemistry of this product, we carried out a DPGSE-NOE experiment. In this experiment, the signal for the proton at C3 was irradiated first. Due to their close proximity in space to the proton at C3, enhancements for the signals of the protons at C9 and C13 are expected for **146**. However, no enhancement was observed for these protons. Then we irradiated the signal for the proton at C7. In this case enhancements are expected for the signals due to the protons at C9 and C13 for **145** but not for **146**. In fact, we did see enhancements for the protons for these signals upon irradiation of the proton at C7 showing that the product is the *1H* isomer **145**, not the *2H* isomer **146** (Figure 28). This outcome is in sharp contrast to that obtained with the 7-NI reaction.

Formation of **145** suggests that the transient intermediate is **148** (Scheme 59). Since, after the formation of the 6-nitroindazolyl anion, the reaction was thought to proceed through intermediates **148**, the unexpected peak appearing at 4.8 minutes earlier in the reaction, was suggested to be this intermediate (Scheme 59).

**Scheme 59. 6-Nitroindazolyl anion attacks 4-chloro-1-methylpyridinium iodide to form intermediate 148, which yields to the product.**



We also wanted to investigate the reversibility of the reaction as it was shown in the case of 7-NI where methyl iodide is captured by TMP to shift the reaction in favor of the N-methyl-TMP adduct (**140**) irreversibly. (Scheme 55)

In this case, we attempted to capture 4-iodo-1-methylpyridinium iodide species **121** at room temperature by introducing the strong nucleophile cyanide. This is expected

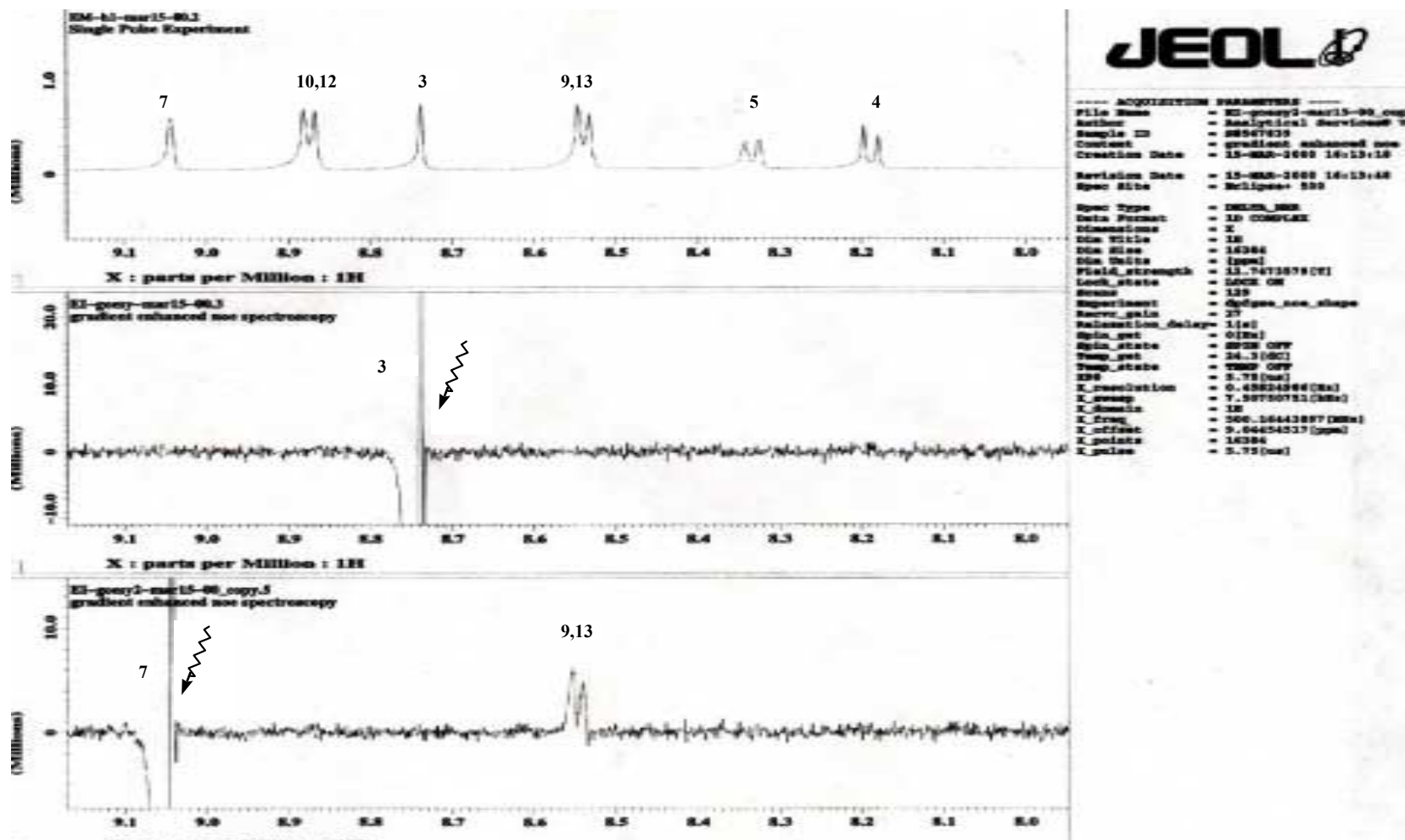
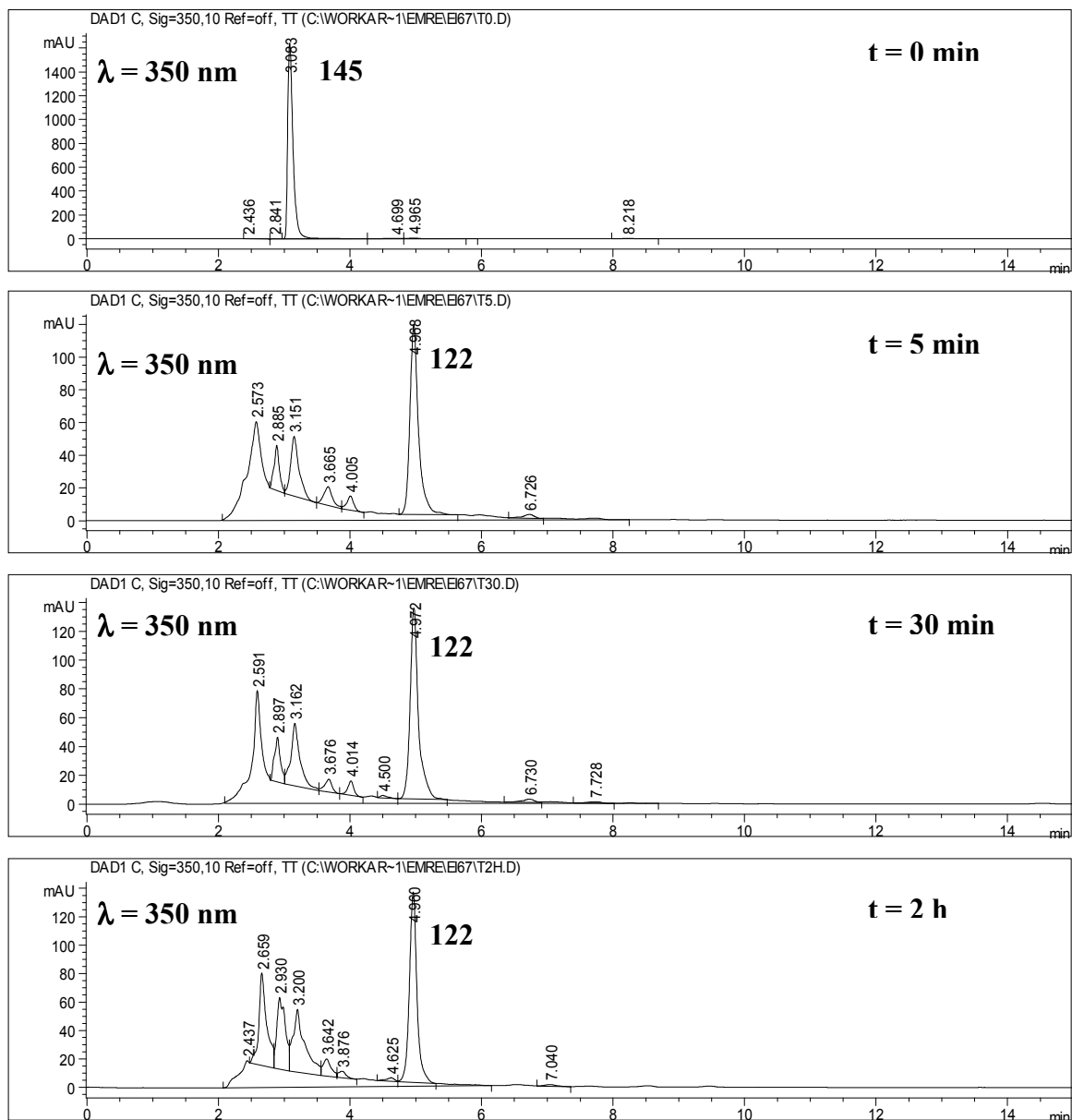


Figure 28. Irradiated  $^1\text{H}$  spectrum of the product 145 or 146.

to introduce the irreversible step which is not possible using TMP at room temperature. Compound **145** was suspended in DMF and an excess of KCN was added to the suspension. HPLC tracings showed that the peak corresponding to **145** disappeared rapidly and was replaced by a peak corresponding to 6-NI. In addition to 6-NI other peaks appeared to form a complicated HPLC tracing (Figure 29).

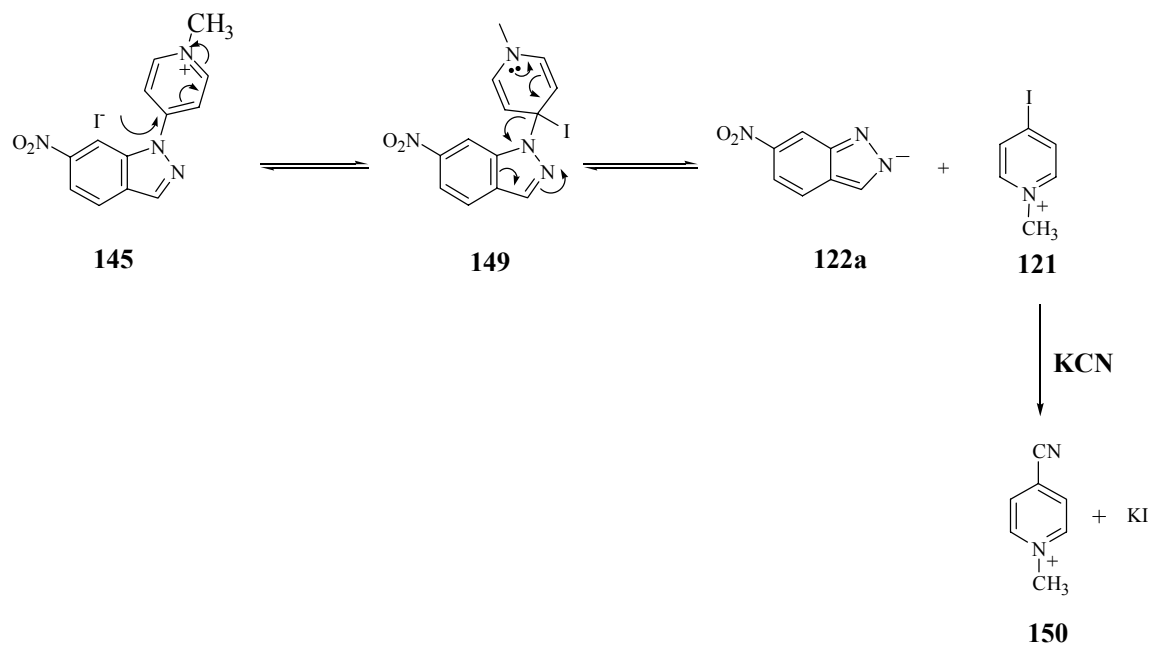


**Figure 29. HPLC monitoring of the reaction mixture containing 145 and excess KCN in DMF at room temperature.**

The peak with the retention time of 3.1 minutes resembled the peak which had been assigned to **121** in Figure 24 where the decomposition of 1-methyl-4-(7-nitroindazol-2-yl)pyridinium iodide (**120**) was monitored.

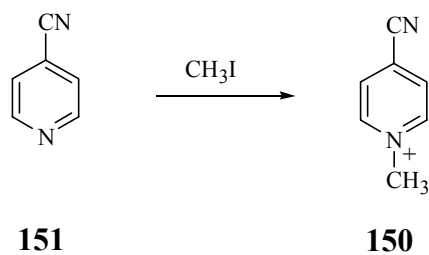
Formation of 6-NI is rationalized by the reaction shown in Scheme 60 where 6-NI leaves with the formation of the 4-iodo-1-methylpyridinium iodide species **121**. This compound then is converted to the stable 4-cyano-1-methylpyridinium species **150**.

**Scheme 60. Cyanide being a strong nucleophile will displace 6-NI in a nucleophilic aromatic substitution reaction forming 4-cyano-1-methylpyridinium (**150**).**



To confirm its formation, **150** was synthesized by treating 4-cyanopyridine with methyl iodide (Scheme 61).

**Scheme 61. Synthesis of 4-cyanopyridinium iodide.**



The HPLC analysis of **150** showed a peak at 2.6 minutes (Figure 30) which is also present in the HPLC tracings in Figure 29 providing evidence for the capture of **121** by cyanide as suggested in Scheme 60 to introduce an irreversible step to the reaction sequence.

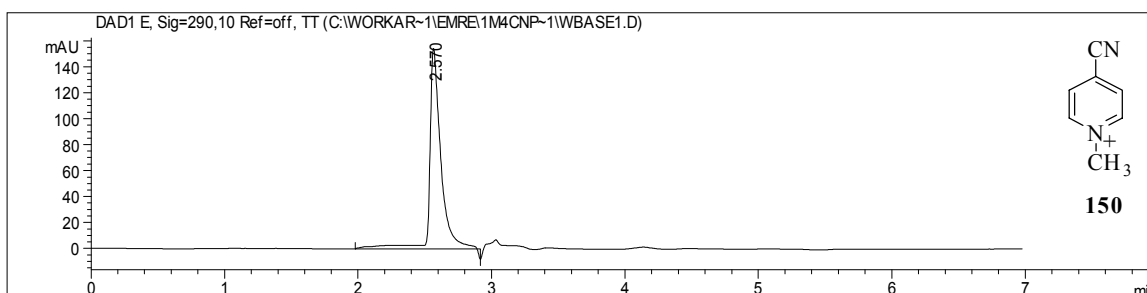
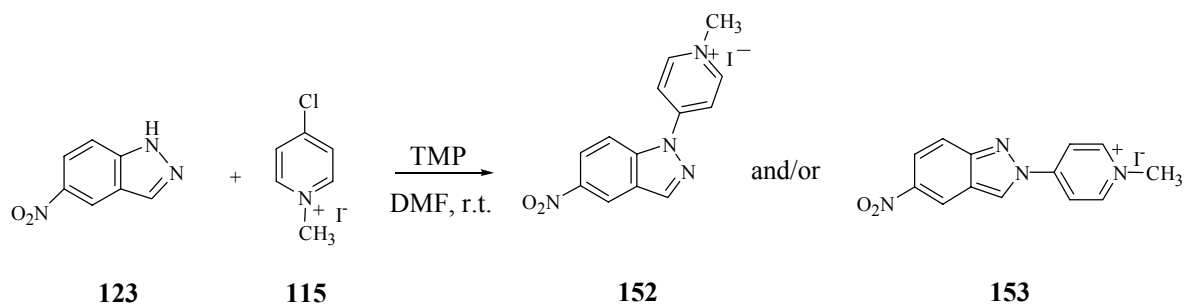


**Figure 30. HPLC analysis of synthetic 4-cyano-1-methylpyridinium iodide **150**.**

The same reaction pathway also was examined with 5-NI (**123**) to generate the corresponding 1-methyl-4-(5-nitroindazolyl)pyridinium iodide species **152** and/or **153** (Scheme 62).

**Scheme 62. Synthesis of 1-methyl-4-(5-nitroindazolyl)pyridinium iodide.**



After the addition of the base, the reaction mixture again turned cloudy after 5 minutes and a solid began to separate. HPLC analysis (Figure 31) showed the disappearance of the peak corresponding to 5-NI (5.0 minutes) and the appearance of product peaks at 3.0 minutes and 3.1 minutes. The solid was filtered after 2 hours and was crystallized from hot methanol to give product in 87 % yield.  $^1\text{H}$  NMR analysis again showed the presence of one isomer only. The HPLC tracing shows the formation of both isomers with a ratio of 2:1. This, however, reflects the product composition in the solution. The high yield we obtained from this reaction suggests that, due to its lower solubility, only one isomer is precipitating. The reversibility of the reaction explains the high yield of the one isomer.

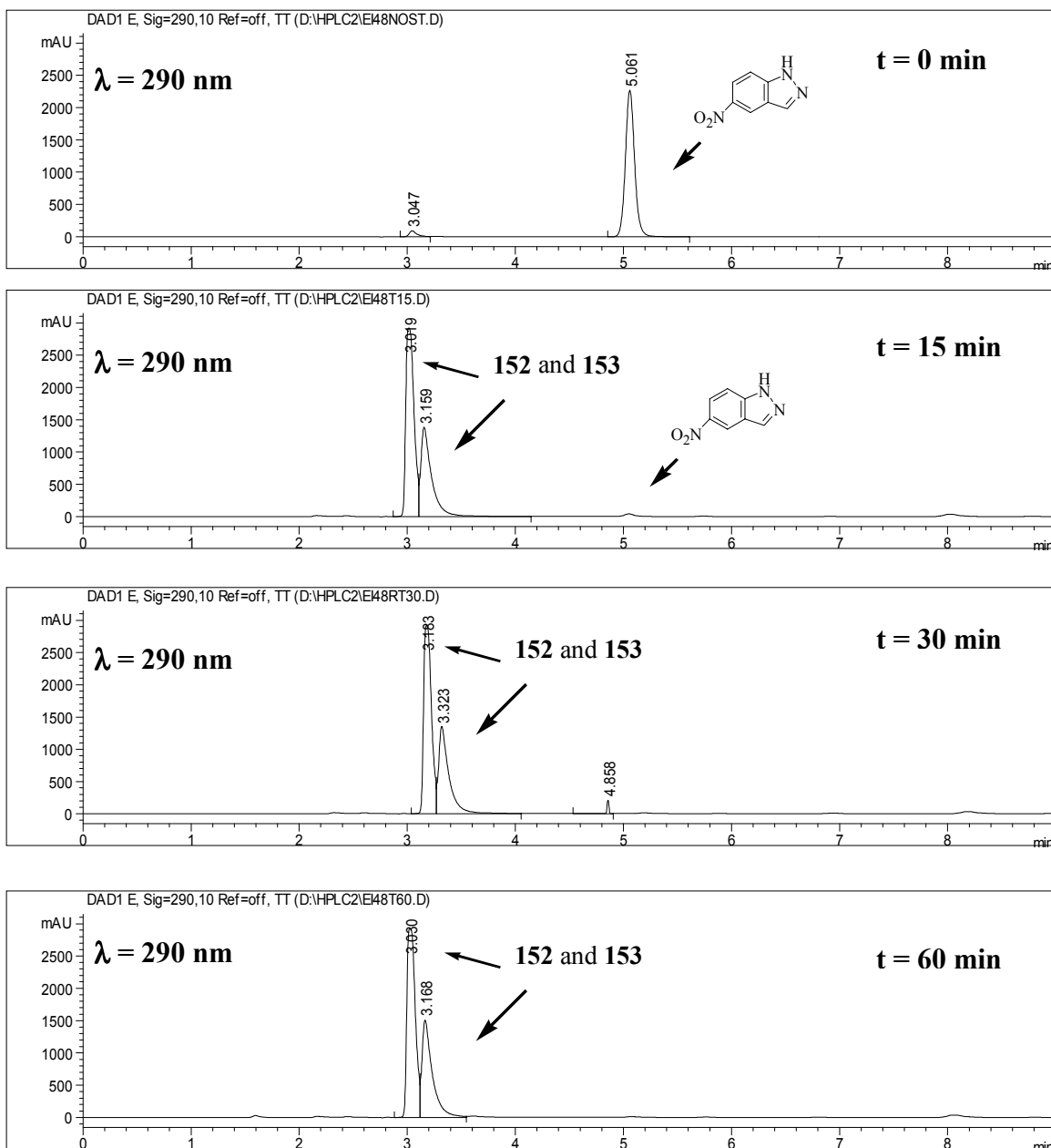


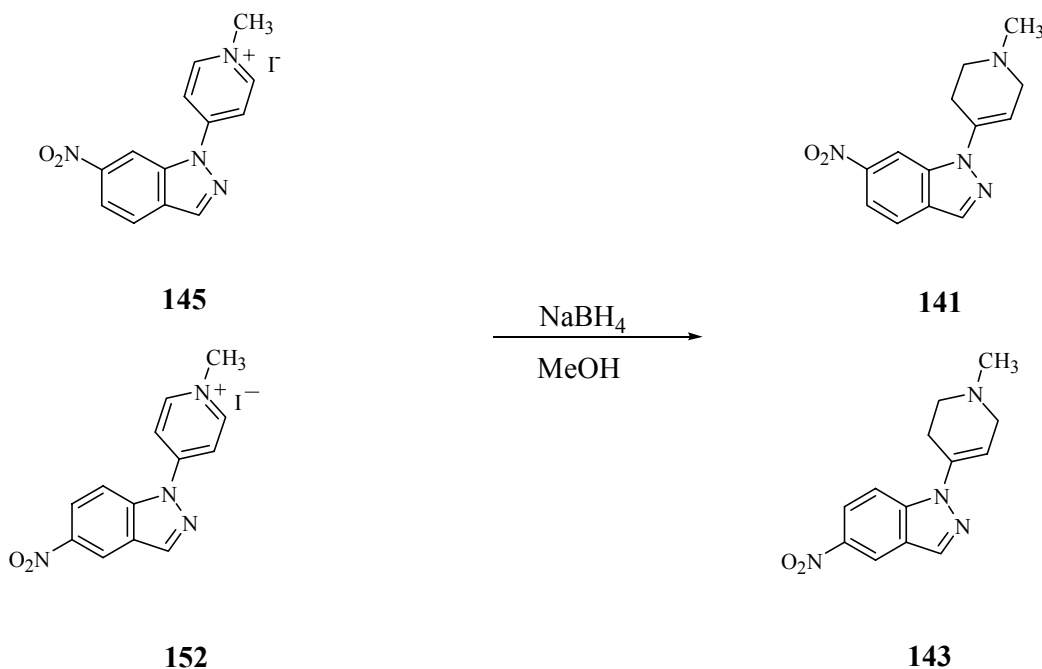
**Figure 31. HPLC monitoring of the reaction shown in Scheme 62.**

A DPGSE-NOE experiment was carried out as described for the 5-NI derived analog to be able to determine the regiochemistry of the product. The NOE effect observed was identical to that seen for **145** establishing that the product is the *1H* isomer **152**.

After the synthesis of the pyridinium compounds, both **145** and **152** were reduced

in methanol using NaBH<sub>4</sub> as the reducing agent to give the potential “prodrugs” of 6-NI and 5-NI, respectively (Scheme 63).

**Scheme 63. Reduction of the pyridinium compounds 145 and 152 to the corresponding tetrahydropyridines to obtain the desired prodrugs 141 and 143.**



### 4.3. REGIOSPECIFIC SYNTHESIS OF 1-METHYL-4-INDAZOLYL-TETRAHYDROPYRIDINES AND ADDITIONAL STUDIES ON THE REACTION MECHANISM

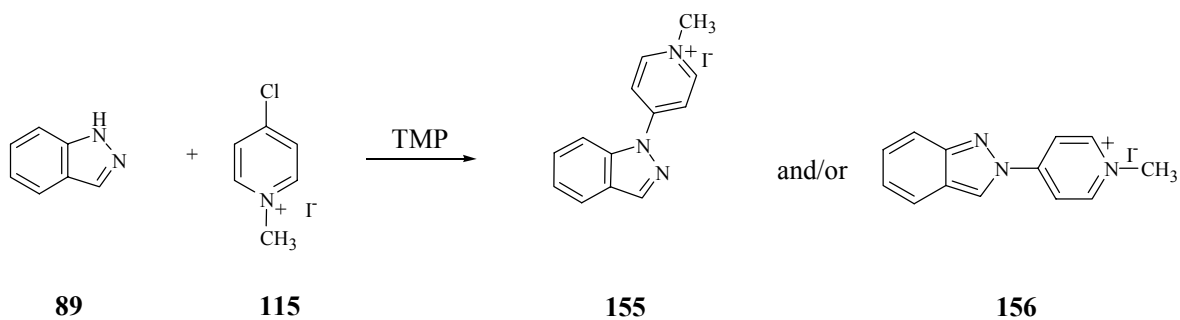
After achieving the synthesis of the “prodrugs” of 5-, 6- and 7-nitroindazoles, we decided to reinvestigate the chemistry with the parent compound indazole (**89**) in an effort to understand better we might understand better the effect of the nitro group on the regiochemistry of the nucleophilic aromatic substitution reaction. The anticipated product(s) of this study, **155** and/or **156**, should help with regiochemical determination of the previously reported pyridinyl precursor **107** or **109** of the “prodrug”.<sup>174</sup>

<sup>174</sup> Reference 144.

### 4.3.1. INVESTIGATION OF THE REACTION

We monitored the reaction of indazole (**89**) with **115** in the presence of TMP at room temperature by HPLC (Scheme 64).

**Scheme 64. The nucleophilic aromatic substitution reaction of indazole with 115.**



After one hour, there was a significant decrease in the intensity of the peak corresponding to indazole and the appearance of two peaks with retention times 3.1 minutes and 3.2 minutes which are assigned tentatively as the isomeric products **155** and **156** (Figure 32). We also observed a small amount of product formation at  $t = 0$  since the aliquot was taken immediately after the addition of TMP.

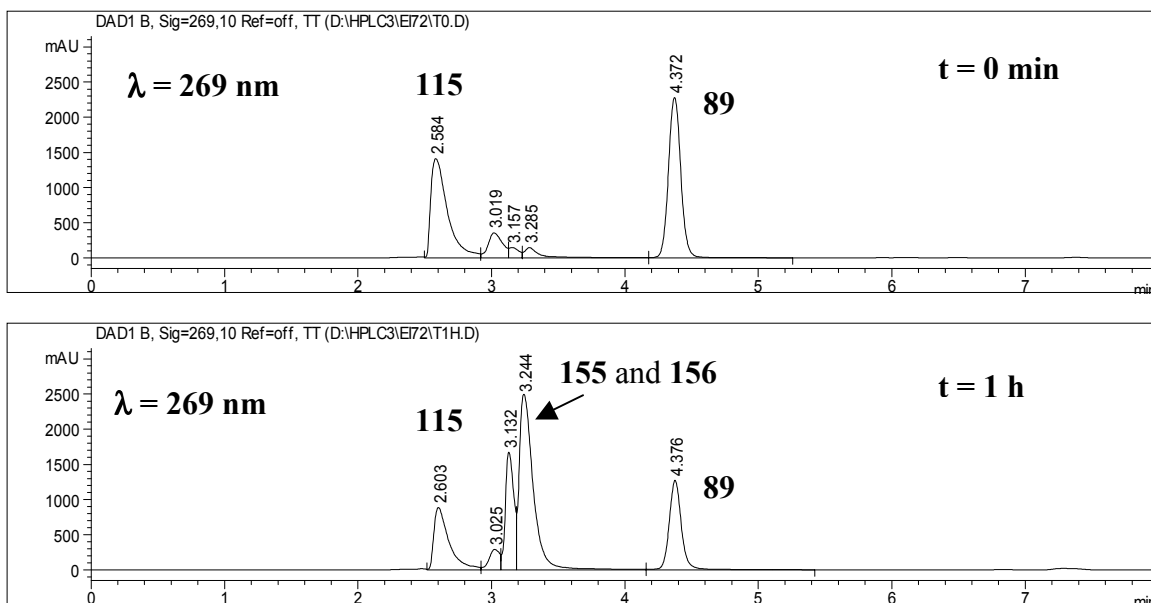


**Figure 32. HPLC monitoring of the reaction illustrated in Scheme 64.**

After 30 minutes, the reaction mixture turned cloudy and crystals began to separate from the solution. After 2 hours, almost all of the starting material was consumed and the progress of the reaction slowed considerably. We isolated the product from the reaction mixture by filtration. The  $^1\text{H}$  NMR spectrum showed a single set of peaks suggesting the presence of a single isomer (See Appendix). The isolation of the minor isomer remaining in the solution was not attempted.

We then carried out a DPGSE-NOE experiment on the product to determine the regiochemistry (See Appendix). We irradiated the signal for the proton at C3 and the only enhancement we saw was for the signal of the proton at C4. There was no enhancement for the signal of the protons at C9 and C13 which would have been the case for the *2H* isomer **156**. Then we irradiated the signal of the proton at C7 and we observed an enhancement for the signal of the protons at C6, C9 and C13 which showed that the product was the *1H* isomer.

#### 4.3.2. NUCLEOPHILICITY OF INDAZOLE COMPARED TO NITROINDAZOLES

Previously, indazole had been reported to react with 4-fluoropyridine (**111**), a compound which should be less electrophilic than 4-chloro-1-methylpyridinium iodide (Schemes 37).<sup>175</sup> However this reaction had failed with 7-NI consistent with the expected decrease in the nucleophilicity of the indazolyl nucleus. Therefore we decided to investigate the requirement of base in the nucleophilic aromatic substitution reaction of **115** with indazole.

We carried out the nucleophilic aromatic substitution reaction between **115** and **89** in the absence of base. HPLC analysis of the reaction mixture did not show any product formation at room temperature or at 60 °C. However, when the temperature was increased to 100 °C, we began to observe the appearance of a single peak. The retention time of this peak, however, corresponded to that of the *2H* isomer, not the *1H* isomer (Figure 33).

---

<sup>175</sup> Reference 144.

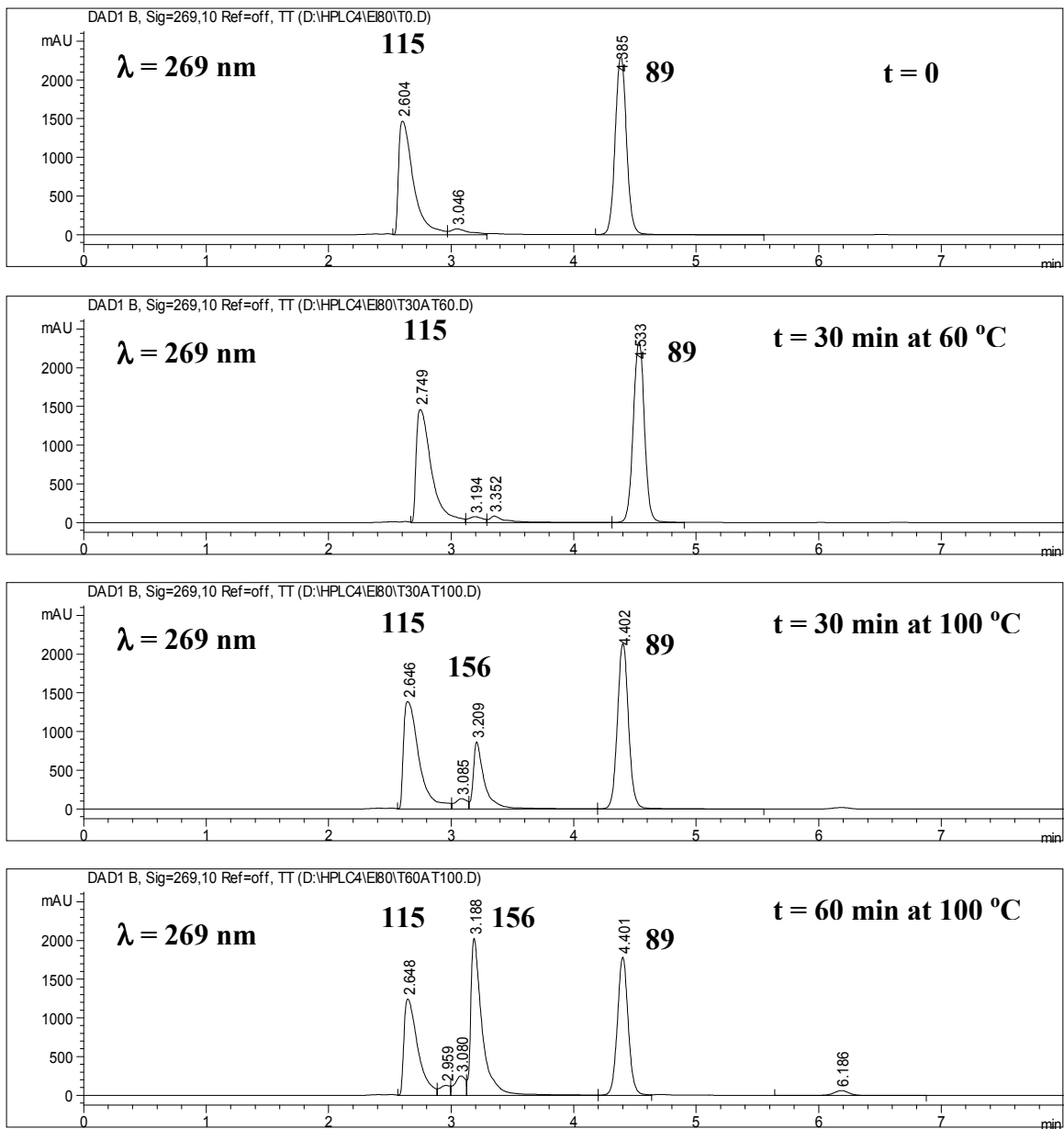


**Figure 33. HPLC monitoring of the reaction illustrated in Scheme 64 in the absence of base.**

After 24 hours, the reaction mixture was cooled down to induce crystallization of the product. The  $^1\text{H}$  NMR spectrum of the filtered crystals in  $\text{DMSO-d}_6$  displayed one set of protons showing the formation of one isomer only (Figure 34).

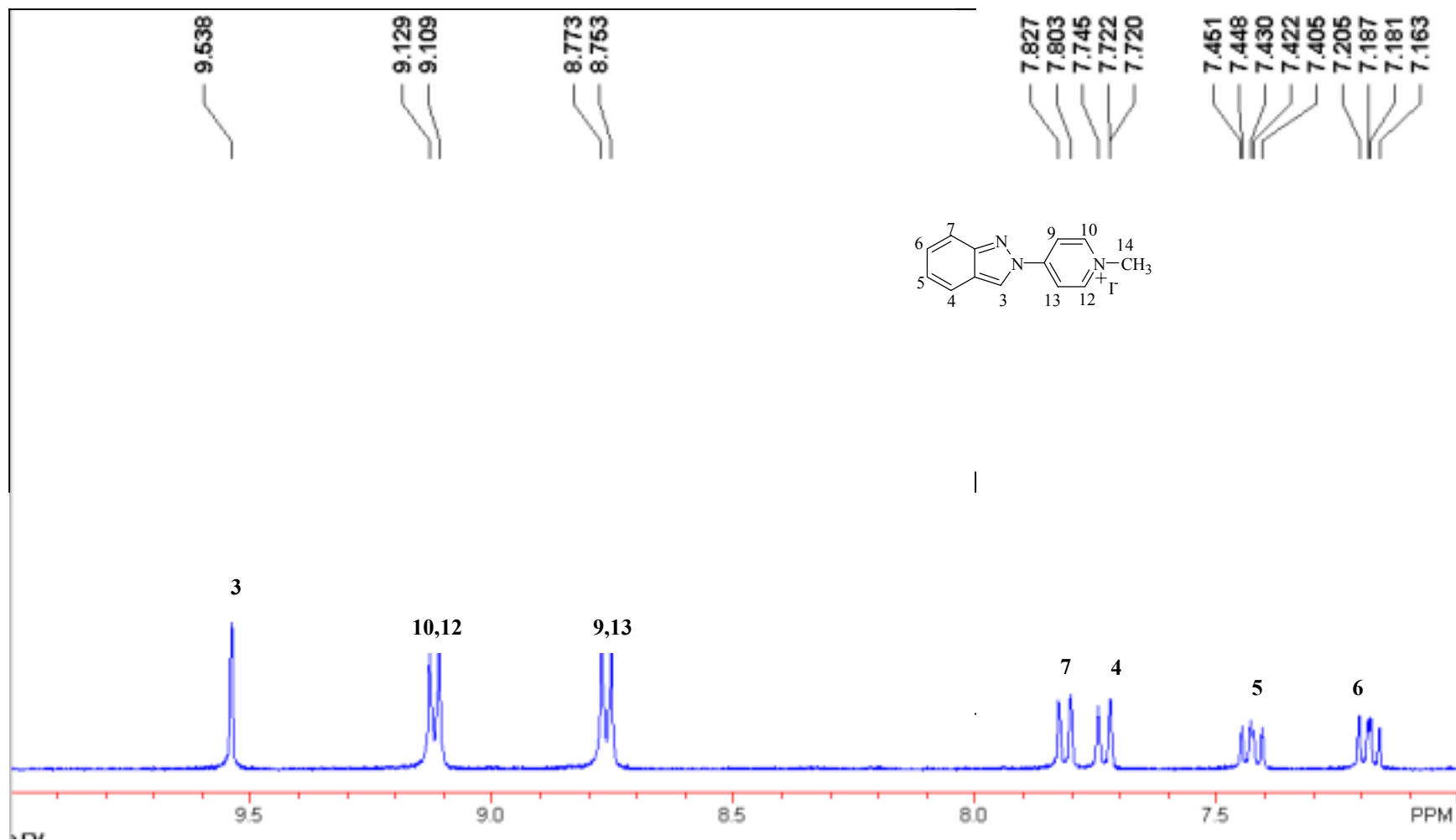
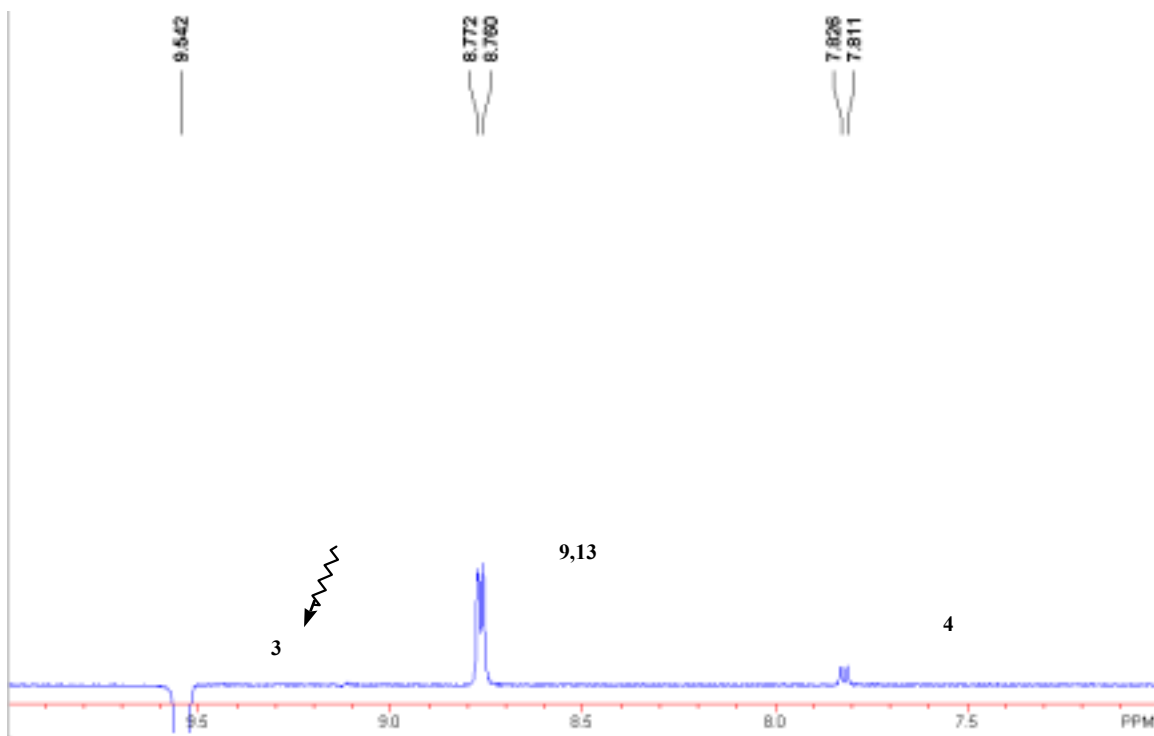


Figure 34. <sup>1</sup>H spectrum (instrument frequency = 360 MHz) of the product obtained from the reaction illustrated in Scheme 64 in the absence of base.

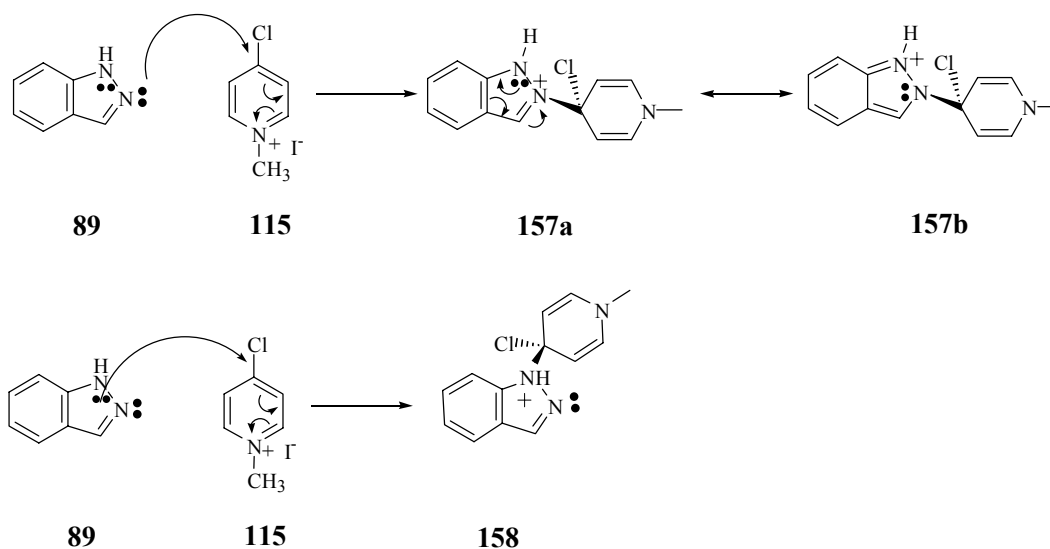
The chemical shifts were significantly different from the *1H* isomer suggesting that the product is the *2H* isomer. In order to confirm the regiochemistry we again carried out a DPGSE-NOE experiment. When the signal for the proton at C3 was irradiated an enhancement for the signal of the protons at C9 and C13 was observed as well as an enhancement for the signal which was assigned to be the proton at C4 (Figure 35). This behavior is fully consistent with the assignment of this product as the *2H* isomer.



**Figure 35. Irradiated  $^1\text{H}$  NMR spectrum of the product obtained from the reaction illustrated in Scheme 64 in the absence of base.**

The exclusive formation of the *2H* isomer in the absence of base can be explained by the better stabilization of the intermediate cation **158** which is not possible in the case of the intermediate leading to the *1H* isomer **155** (Scheme 65). The energy barrier leading to the *1H* isomer is most likely higher. In the presence of base, the intermediates leading to the *1H* or the *2H* isomers are both neutral species. The energy requirement is lower and the reaction can take place at room temperature. Although, in this case both intermediates are of similar energy, the higher thermodynamic stability of the *1H* product **155** dictates the outcome of the reaction.

**Scheme 65. Stabilization of the intermediate 157 formed in the absence of base which is not possible for the localized cation 158.**



However, in the case of nitroindazoles, the nucleophilicity of N2 is lowered due to the electron withdrawing effect of the nitro group. Due to this decrease in nucleophilicity, the use of base was required in the case of nitroindazoles since only the corresponding anion is adequately nucleophilic to attack **115**.

Finally, to have a complete understanding of the reaction mechanism, we studied the possibility of altering the reversibility of the reaction by introducing an irreversible step as we observed for the nitroindazoles. The *2H* isomer **156** was heated in DMF to 60°. After 30 minutes, HPLC analysis did not show any changes. The temperature then was increased to 100°C and then to 150°C. However, there was still no change in the composition of the reaction mixture.

According to our understanding of the reaction mechanism with nitroindazoles, base was needed to induce an irreversible step in the reaction pathway. Therefore we included TMP and again heated the *2H* isomer in DMF. After heating the *2H* isomer for 30 min at 60°C, analysis of the reaction mixture by HPLC showed the appearance of a peak which has the same retention time and identical UV spectrum as those of the *1H* isomer. The appearance of the peak for **155** was paralleled by disappearance of the peak corresponding to the *2H* isomer **156** (Figure 36).

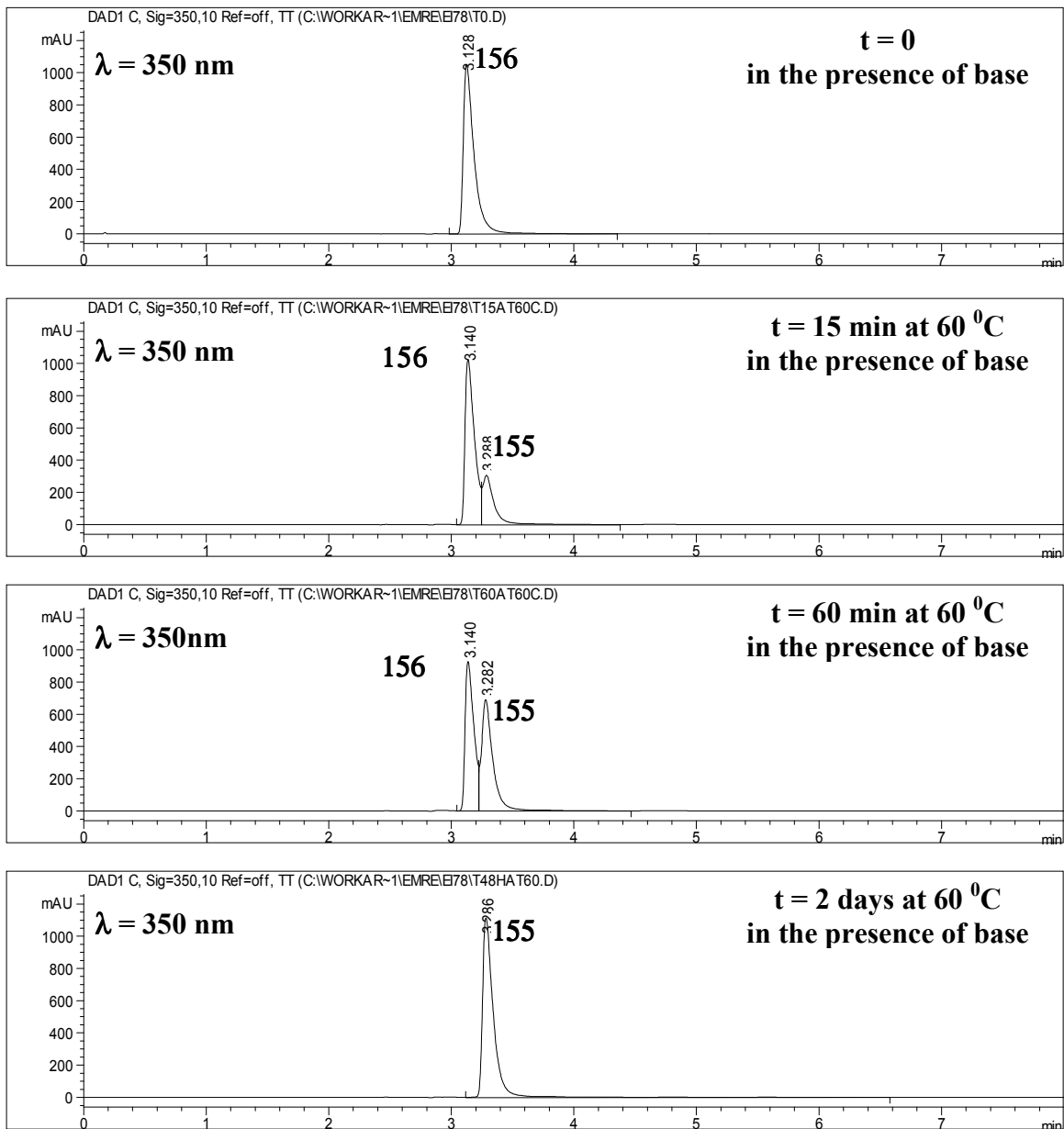
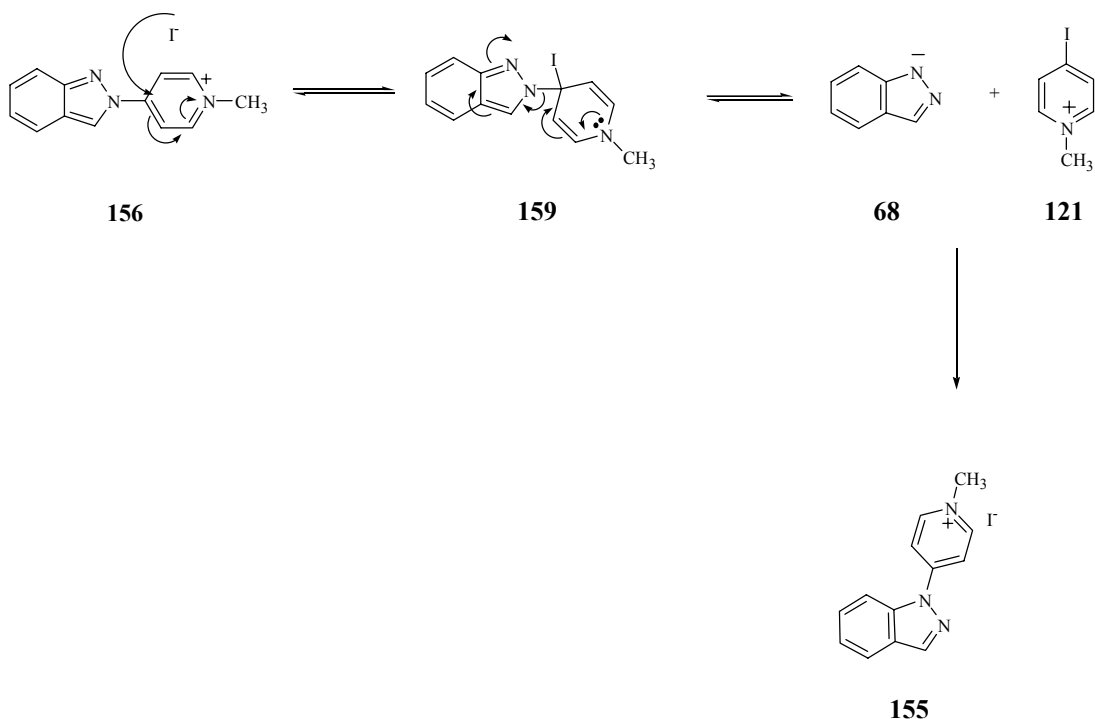


**Figure 36. HPLC monitoring of the isomerization of 156 to 155 at 60 °C in the presence of TMP.**

The same attempt in the case of 1-methyl-4-(7-nitroindazol-2-yl)pyridinium iodide (**120**) had resulted in decomposition instead of isomerization to the *IH* isomer. However with 1-methyl-4-indazol-2-ylpyridinium iodide (**156**), isomerization to the

thermodynamically more stable *IH* isomer was favored over the decomposition reaction. To account for this isomerization we propose the mechanism shown in Scheme 66

**Scheme 66. Isomerization of 1-methyl-4-(indazol-2-yl)pyridinium iodide (156) to 1-methyl-4-(indazol-1-yl)pyridinium iodide (155).**



After the attack by iodide, intermediate (159) is obtained. This intermediate can cleave to form indazolyl anion (68) and 4-iodo-1-methylpyridinium iodide (121). Indazolyl anion can either react with 121 to form the more stable isomer 155. In the absence of base it is possible that, the small amount of indazolyl anion (68) forming, reacts with the trace quantity of water present in the reaction mixture to give indazole. The reaction of indazole with 121 will again form the *2H* compound 156.

Consistent with this analysis thermodynamically more stable *IH* isomer 155 did not rearrange to the *2H* isomer 156 under these conditions (Figure 37).

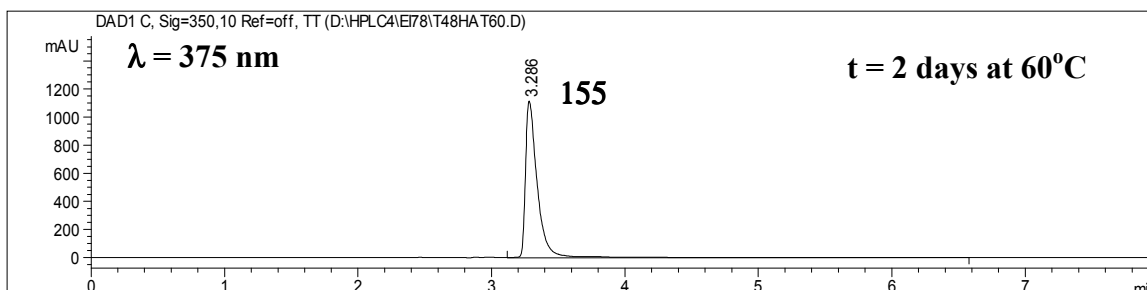


**Figure 37. HPLC tracing obtained after heating 155 for 2 days in DMF at 60 °C.**

These results provided us with a better understanding of the reaction mechanism of the nucleophilic aromatic substitution reaction of indazole, as well as a simple and efficient way to synthesize regiospecifically 1-methyl-4-indazolylpyridinium iodides **155** and **156**.

#### 4.3.3. SYNTHESIS OF PRODRUGS OF INDAZOLE

In order to synthesize the “prodrugs” of indazole we carried out the reduction of **155** and **156** to the corresponding tetrahydropyridines **160** and **161** (Scheme 67).

**Scheme 67. Reduction of 155 and 156 to the corresponding tetrahydropyridines 160 and 161.**

